REPORT NO. P65-49

FINAL REPORT – APPENDIX, VOLUME II

THE STUDY OF MULTIPACTOR BREAKDOWN IN SPACE ELECTRONIC SYSTEMS

NATIONAL AERONAUTICS AND SPACE ADMINISTRATION
GODDARD SPACE FLIGHT CENTER

CONTRACT NAS 5-3916

APRIL 1965

GPO PRICE $ _____

CFSTI PRICE(S) $ _____

Hard copy (HC) $3.00

Microfiche (MF) .25

ff 653 July 65

AEROSPACE GROUP

HUGHES

HUGHES AIRCRAFT COMPANY
CULVER CITY, CALIFORNIA

FINAL REPORT -- VOLUME II

THE STUDY OF MULTIPACTOR BREAKDOWN IN SPACE ELECTRONIC SYSTEMS

APRIL 1965

RESEARCH AND DEVELOPMENT DIVISION
AEROSPACE GROUP
Hughes Aircraft Company . Culver City, California

TABLE OF CONTENTS

PART I

PRECAUTIONS IN DESIGN TO AVOID MULTIPACTOR PROBLEMS

PART I. PRECAUTIONS IN DESIGN TO AVOID MULTIPACTOR PROBLEMS

I. Potential Problems of Space Electronic Equipment Due to Multipactor

The following problems may be of concern to designers of spacecraft radio frequency equipment.

A. Voltage Breakdown Due to Gas Ionization Caused by Multipactor Outgassing

The voltage breakdown due to multipactor is evidenced by a pale blue glow, which is not visible under daylight illumination. It usually represents a low power dissipation on the surfaces affected, perhaps never greater than 20 MW/CM^2, and an equivalent impedance of low power factor of a magnetitude which may be smaller than 1000 ohms for a heavy discharge across a large plate areas such as 20 square inches. If the discharge is "weak", the shunt impedance will be very high. Two indirect difficulties may result from the multipactor discharge (a) detuning and (b) evolution of gas. The detuning effect will be significant for high impedance circuits and negligible for low impedance circuits. The evolution of gas may be a very serious problem. Since there may be a gas ionization breakdown in the strong r.f. field which produced the original multipactor, and since gas discharges can absorb substantial amounts of power, they may lead to catastrophic failure and physical damage. Substantial percentages of the r.f. power available are dissipated in such gas ionization breakdown, and arcs between low voltage d.c. terminals have also been observed. The gas ionization breakdown appears to be the major source of failures observed to date.

B. Power Loss, Heating, Gas Evaluation Without Breakdown

Although a multipactor breakdown may exist and should be a matter of concern to the designer, it may not require corrective action. As noted in item A above, the power loss, heating, and gas evolution due to the multipactor glow, itself, do not ordinarily represent conditions of failure. In particular, if the gas evolved is vented or pumped away so that the local pressure cannot rise to a level which would support

breakdown, the power loss and heating effects will usually be small enough to be tolerated. Of course, the multipactor discharge is a plentiful source of electrons and ions which may cause troubles with certain types of scientific experiments. In addition, we have observed surface discoloration probably due to outgassing and redeposit of material on surfaces adjacent to the discharge; such effects might be damaging to optical equipment. Some form of the mechanism of sputtering may occur in the presence of d.c. fields.

C. Noise and Harmonic Generation

Measurements indicate that the multipactor discharge contains noise currents which are several orders of magnitude larger than thermal, across the tuned circuit in which they have occurred. In a high or medium power transmitter this effect will usually be negligible except for the possibility that a transmitter will be operated, simultaneously, at a frequency near the frequency of the system receiver. Tests reported in the Final Report of Contract NAS 5-3916, indicate approximate values measured for a 12 megacycle spacing with a 100 megacycle discharge.

Since the multipactor discharge is produced, between parallel plates, by a flat sheet of electrons which oscillate back and forth in resonance with the electric field, the current is nonlinear and contains harmonic components. Typical measurements show content greater than 10% for second and third harmonic; measurement accuracy was not good enough to yield useful results for higher order harmonics but these are probably also present. Since most transmitter power output stages are not highly linear, anyway, the harmonic content of the multipactor discharge should not create problems. However, if the discharge occurs in a component beyond the RFI harmonic filter, such as the antenna system or feed cables, the harmonic content would be radiated directly.

D. Cross Modulation, Intermodulation

A likely place for a multipactor discharge to occur is the antenna or diplexer of a transmit/receive system. Should this occur there is high probability of cross modulation of transmitted and recieved

signals as well as intermodulation of the transmitted spectrum due to the nonlinear character of the multipactor effect. Noise in the discharge may appear at the input of a sensitive receiver by this mechanism, also.

II. Prediction of Multipactor

A. Introduction

Part II of this Handbook offers curves and experimental data of a specific nature. Part III of this Handbook contains theoretical background, as does the Final Report itself. The qualitative considerations are described herewith.

B. Geometric-Voltage Resonance Conditions - Parallel Plates

Multipactor discharge occurs when the electron transit time due to the radio frequency electric field is approximately resonant with the applied frequency, or with one of its harmonics. For parallel plates, a product f x d (frequency in megacycles X spacing in centimeters) of the order of magnitude of 100 will probably allow a multipactor discharge to exist when the applied voltage is greater than a few tens of volts. A thorough theoretical discussion of this relationship is given in Part III.

A single surface multipactor can also exist. This phenomenon occurs when the two plates are used with a d.c. bias as well as the applied r.f. field; the electron paths, in this case, originate and terminate on the same plate, and consequently, the secondary emission characteristics of the plate which is not struck by electrons do not influence the result.

C. Coaxial Multipactor

Single and double surface multipactor discharges have been observed in coaxial cylinders. When the spacing between the cylinders is small compared to the average radius, the behavior of the discharge follows a voltage resonance equation much like that of the parallel plate case. Since the voltage is a function of the product of diameter and frequency, these curves may be used at any frequency. Furthermore, multipactor is observed with small inner cylinders; the kink in the curves may be due to existence modes of resonance in which electrons traverse a path length nearly

along a diameter of the outer cylinder without collision with the inner cylinder.

D. Other Modes

As indicated in Part III, multipactor discharges may occur along paths influenced by magnetic fields, in waveguides, in waveguide slots, and, in general, almost anywhere there is a path along which electrons may be accelerated in a vacuum by a radio frequency field.

E. Secondary Emission Characterisitcs

A necessary condition for sustained discharge is that the net secondary emission ratio for the multipactor surfaces should be greater than 1. Since materials have wide variability of secondary emission ratio, the conditions which initiate multipactor are sensitive to the nature of the surface. Furthermore, the secondary emission ratio is a function of the arrival energy of the electron, increasing from a small value at low arrival energy and exceeding 1.0 only for some minimum value. The minimum value is a function of the surface characteristic. For common materials, tested in this program, we have observed that minimum arrival energies of 15-20 electron volts are effective in producing discharge. These values are believed to be lower than those assumed by other investigators, and can be used for conservative design calculations.

The analysis and theory which is propounded in the Final Report and in Part III is based on a semi-empirical solution of a differential equation. In these equations, it is assumed that there is a relationship between the arrival energy (velocity) of an electron and the emission energy (velocity) of the resultant secondary electron. This is not true, in fact. The emission energy is nearly independent of arrival energy and has a statistical distribution with a maximum at approximately 10 electron volts.

III. Methods of Eliminating Multipactor

A. Pressurization

Multipactor does not occur in systems where the length of the discharge path is large compared to the mean free path of electrons. In almost any spacecraft environment, the mean free path is usually large enough; however, by maintaining the ambient pressure above 10^{-3} mm, the likelihood of multipactor is reduced to the vanishing point. Since gas ionization is, however, a possibility at such pressures, it is necessary to maintain the ambient pressure at least in the range of one atmosphere. By this technique, the multipactor problem may be replaced by the mechanical problem of sealing a unit, testing its leakage, and maintaining the seal over long periods of time. Since the radio frequency energy must ultimately be launched into space, there is an interface to a vacuum environment in every spacecraft system; frequently, it is possible to eliminate multipactor at such an interface more easily that it can be done in the high power stages of the transmitter.

B. Use of Foam

It has been shown that typical spacecraft foam is capable of lowering the mean free path length to an extent that multipactor is almost always suppressed. We have found that it is not easy to prevent slight discharges or slight local heating inside the volume enclosed by foam. When gas is evolved by such heating, a destructive gas ionization breakdown may occur. The crucial problem is to vent or pump out the internal gas molecules so rapidly that destructive breakdown cannot occur. Foams with communicating cells are essential, and, in addition, the orifices open to vacuum must have adequate cross section to allow rapid diffusion of the molecules.

C. Solid Dielectric Materials

It has been shown that surface coatings of sheet teflon, expoxy resin, and Dow Corning vacuum grease tend to raise the initial voltage at which multipactor starts by a factor between one and two times the uncoated value. However, the discharge is not absolutely

preventable by this technique. It may be possible to suppress multipactor by complete filling of the voids with dielectric material; in this procedure, the same caution must be observed, as with foam, to avoid accumulation of local gas pressure.

D. Bias

D.C. bias voltage applied between multipacting surface points is effective in eliminating the discharge within limits explained in Part III of the Handbook.

E. Control of Geometry

The dimensions of the system can be controlled to avoid values which satisfy the resonance equation. At high radio frequencies this may or may not be feasible, since some circuits must have dimensions comparable to a fraction of a wavelength, it is noteworthy that spacings can sometimes be made too small to satisfy the breakdown conditions of resonance.

IV. Test Procedures for Evaluating Equipment

A. Methods of Detecting Discharge

1. Due to the inevitable presence of residual gas ions, the multipactor discharge always produces at least a faint glow. This is not visible in ordinary laboratory illumination but usually can be seen with naked eye in darkened lab, and can be photographed with ordinary film.

2. Phosphorescent material, such as zinc sulfide, tends to glow when it is bombarded by electrons, and therefore, is useful as a multipactor indicator. The persistence of the phosphor glow and the possibility of secondary emission from it are undesirable.

3. Electron, Ion Collector Plates

The most sensitive detector of multipactor which we have used is a collector electrode placed in the vicinity of the discharge. A positive or negative bias results in a d.c. current flow to the electrode which can be measured with a sensitive current meter; to the best of our knowledge, a significant current flow has always been associated with a multipactor discharge.

B. Vacuum Environment of Tests

1. Unfortunately, most test fixtures and surfaces used for multipactor research will liberate gas under the bombardment of electrons and the heating effect of the discharge. Typical vacuum environments are actually contaminated by absorbed material on the surfaces of test fixture and by pump oil vapor or other material. For these reasons, it is not easy to maintain constant conditions during a test. In addition, the bell jar or vacuum chamber does not simulate perfectly the real space environment.

2. One unique problem which has been found in the course of one study is that the liberated gaseous material is redeposited on the surface in the vicinity of the multipactor and thereby causes significant change in the surface properties. For example, a discharge initiated at a pressure of 10^{-6} mm may simply disappear while simultaneously the chamber pressure rises to 10^{-5} mm. However, we have not invented a method of eliminating multipactor at all. It happens that a restoration of the chamber pressure to atmosphere or continued pumping to very hard vacuum may regenerate the surface so that it will once again sustain a discharge when retested.

The treacherous aspect of this behavior is that it may be possible to perform a test during which the discharge will vanish and not be detected even though it may return again under conditions of actual use.

Test performed with very hard vacuum, such as 10^{-5} mm or less, tend to produce discharges which are stable over a long period of time and can be initiated and extinguished with a good degree of consistency.

The importance of accurate test environmental simulation, including the venting effects of all openings and channels which may be present in the spacecraft itself, is evident from the preceding discussion of gas ionization breakdown which may be induced by multipactor.

PART II

REFERENCE DATA FOR DESIGN

MEAN FREE PATH OF ELECTRONS

Using the table below, and the relationship that mean free path of electrons is inversely proportional to pressure, one can calculate whether or not conditions are suitable for multipactor. If the mean free path is long compared to the physical dimensions of the affected volume, multipactor is possible.

The classical analysis for λ, the mean free path, shows that there is an exponential decrease with distance in the number of molecules which have not suffered collisions after traveling out from an origin; the value, λ, is the distance at which 37 percent (1/e) of the molecules will have had no collisions. At a distance of 4λ, only 2 percent of the original molecules will have had no collisions. The mean free path of an electron, λ_e, is calculated to be $4\sqrt{2}\,\lambda$ when it is present in a gas filled volume, the mean free path of the electron being longer because of its smaller cross section. In general, the mean free path of molecules and electrons is inversely proportional to pressure. The mean free path of representative gas molecules and electrons is given below in Table I.

Pressure, mmHg	Gas Molecule	Molecule Mean Free Path λcm	Electron Mean Free Path λ_e cm
10^{-3}	He	17	96
10^{-3}	Ne	12	68
10^{-3}	A	8	45
10^{-3}	N_2	6.7	38
10^{-3}	K_r	6.6	37
10^{-3}	C_s	0.14	8

Table I. Molecular and electron mean free path at 0°C.

BASIC EQUATION FOR PARALLEL PLATE MULTIPACTOR

The equation given below permits a preliminary calculation which will indicate if the dimensions, frequency, and applied voltage are suitable for multipactor. More complete experimental data is given elsewhere.

The equation for resonance is

$$V = \frac{\omega^2 d^2}{\left(\frac{e}{m}\right)\Phi} \quad \text{or} \quad d = \frac{1}{\omega}\sqrt{V\Phi\left(\frac{e}{m}\right)} \tag{1}$$

$$\Phi = \left(\frac{K+1}{K-1}\right)\pi \cos\phi + 2\sin\phi \tag{2}$$

where

- V = the voltage for secondary emission electron resonance, one half cycle mode
- ω = angular frequency
- d = plate spacing
- $\frac{e}{m}$ = a well known physical constant of the electron
- K = ratio of electron arrival velocity to component of emission velocity in the direction of the electronic field
- ϕ = phase angle (with respect to RF field) at which secondary electron is emitted

Φ is a function of both K and ϕ, neither of which may be predicted theoretically. Limiting values of Φ are determined empirically by fitting of experimental observations. Typically, K is of the order of 4, and $-60° < \phi < 18°$. For these limits Φ varies between 0.77 and 5.44.

Figure 3(a) indicates the definition of terms shown in Table II. In order to sustain multipactor the product of the values of δ for all surfaces involved must be greater than one. Values in the table refer to relatively clean surfaces. Our experimental results indicate that ordinary surface cleanliness results in values of W_f as low as 15-20 eV for many materials. Figure 3(b) indicates the dependence of δ on angle of incidence.

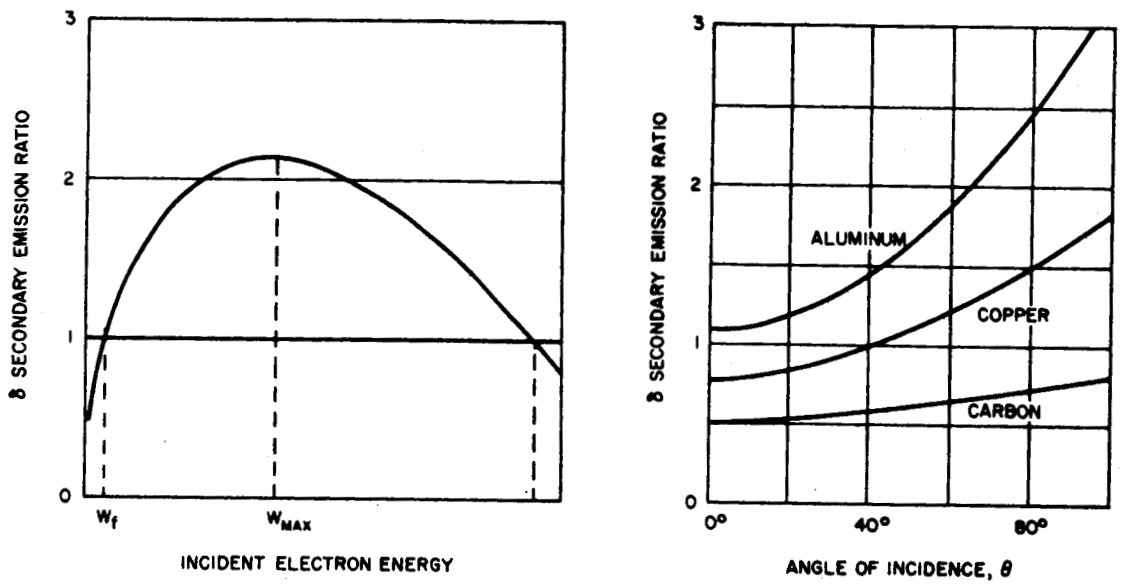

(a) δ vs. W (b) δ vs. θ

Figure 3. Secondary emission parameters.

Material	$W_{\delta = \delta_{max}}$ (eV)	δ_{max}	W_f (eV)
Copper	600	1.3	75-175
Mica	380	2.4	30
Quartz	400	2.1	30
NaCl	600	6.8	15
Al_2O_3	350	2.5	20
Fe	350	1.3	125

Table II. Secondary emission ratio as a function of electron energy.

BREAKDOWN VOLTAGE FOR COMMON MATERIALS
PARALLEL PLATES

These curves may be used for frequencies other than those listed for the experimental data, since the governing parameter is f x d.

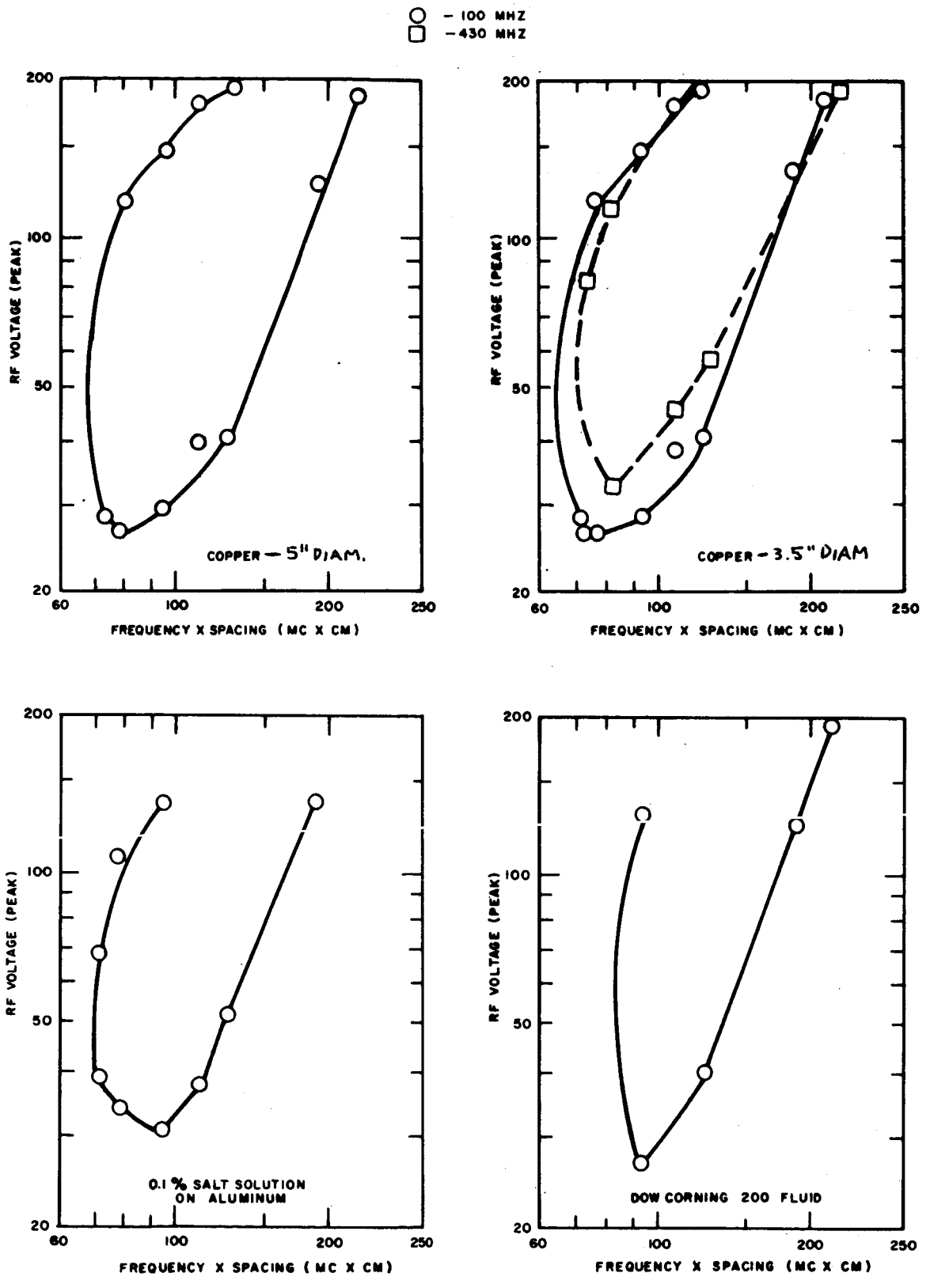

BREAKDOWN VOLTAGE FOR COMMON MATERIALS
PARALLEL PLATES

These curves may be used for frequencies other than those listed for the experimental data, since the governing parameter is f x d.

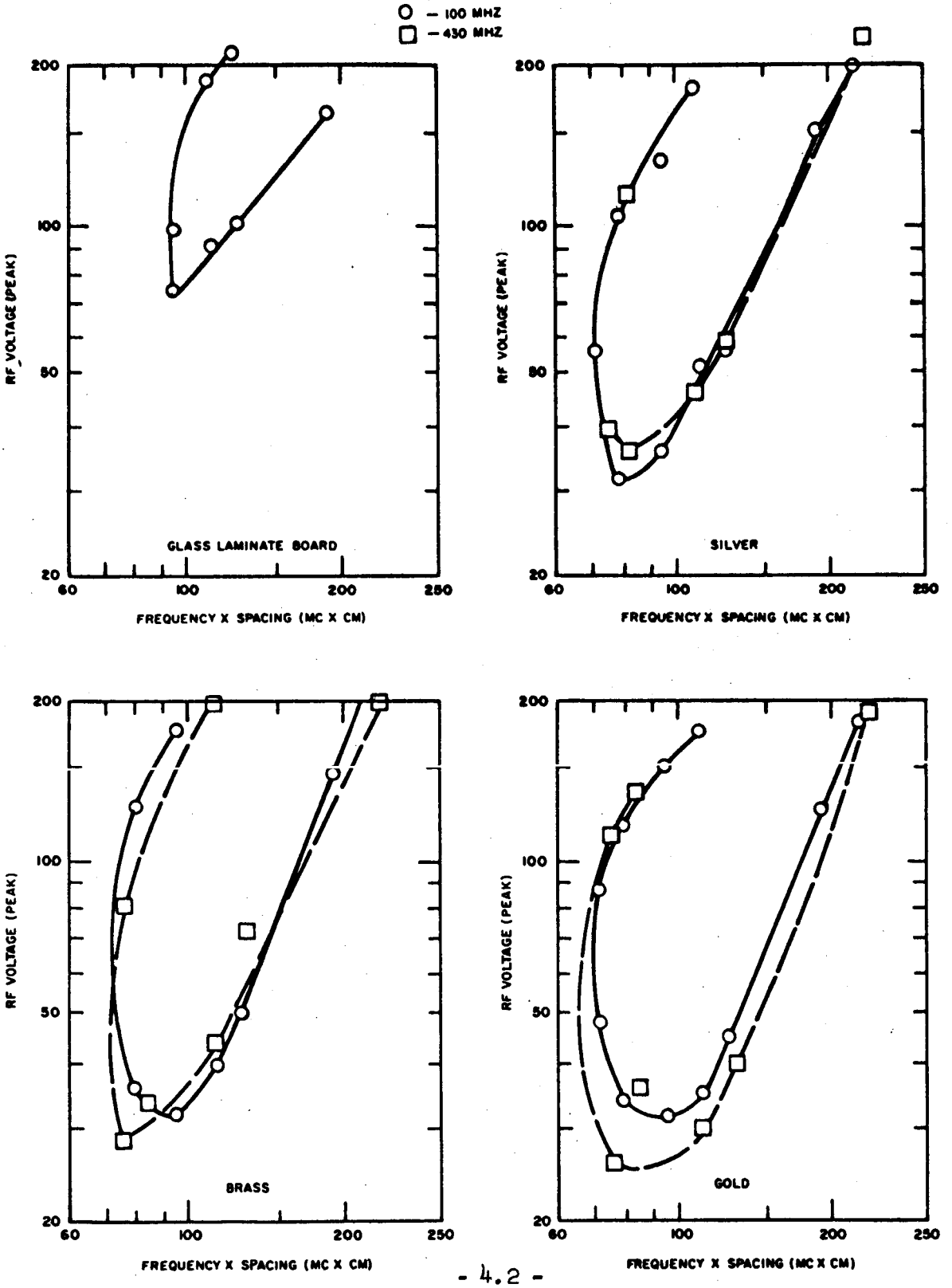

BREAKDOWN VOLTAGE FOR COMMON MATERIALS

PARALLEL PLATES

These curves may be used for frequencies other than those listed for the experimental data, since the governing parameter is f x d.

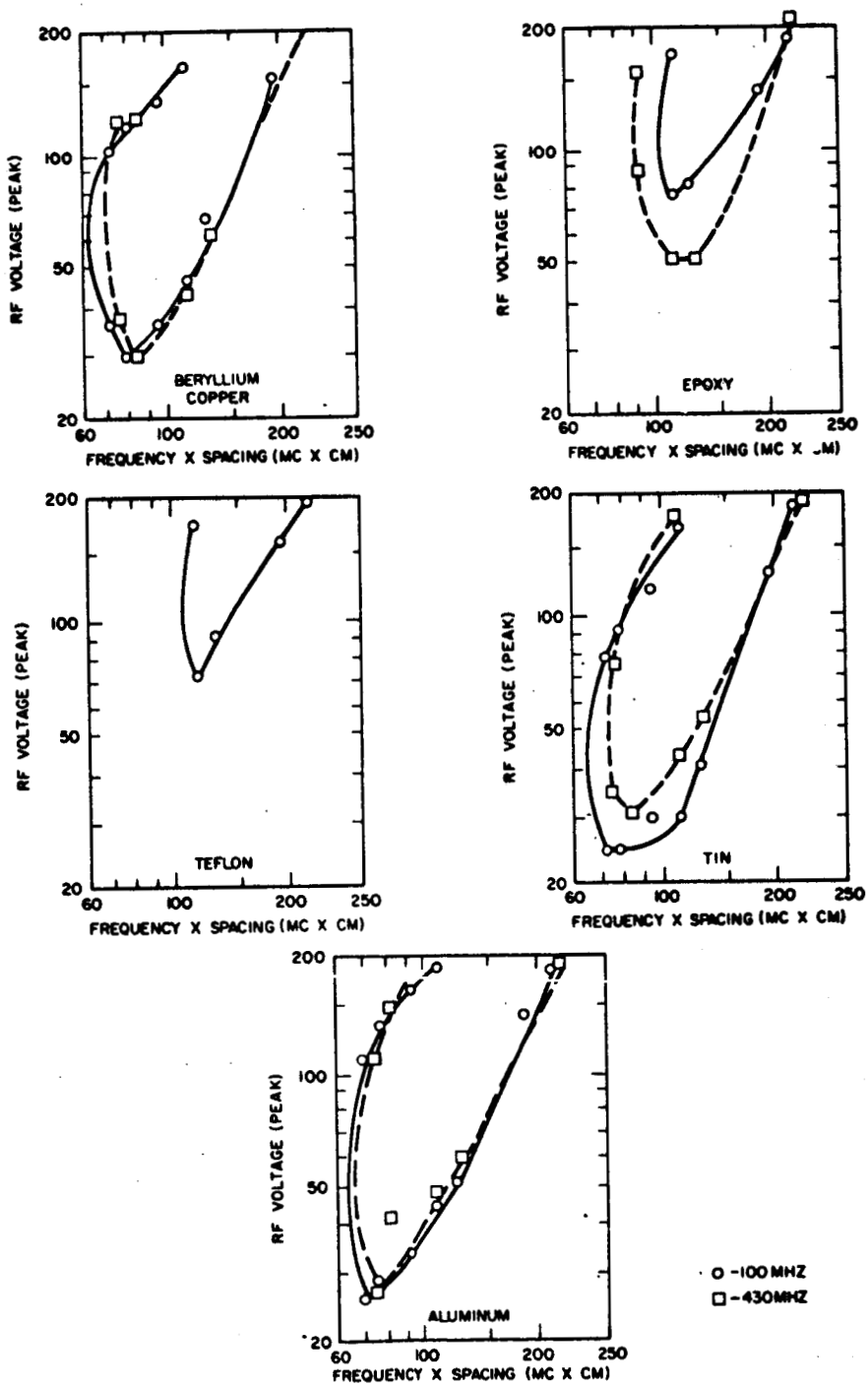

MINIMUM BREAKDOWN AND ARRIVAL ENERGY FOR
MULTIPACTOR BREAKDOWN OF COMMON MATERIALS

Each plotted point in the figure below represents an experimental measurement. It is important to note that many observations have shown arrival energy in the 15-30 eV range, which is far below the threshold value reported by some experimenters.

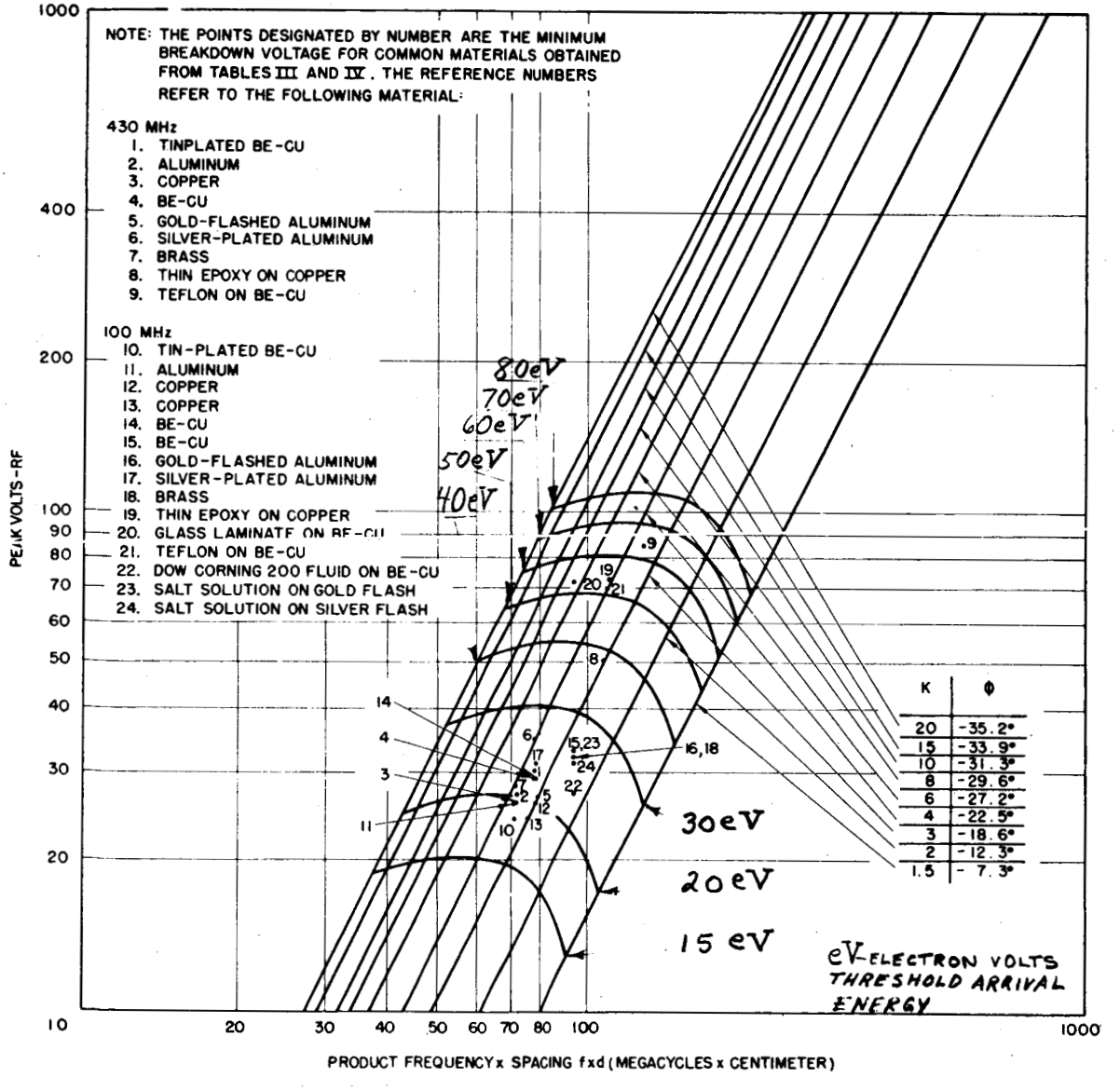

BREAKDOWN VOLTAGE FOR 50 OHM COAXIAL CYLINDERS

The coordinate points represent experimental data taken at 430 mc, while the other curve is based on both an extrapolation of data from parallel plate measurements and on isolated points measured at 100 mc, and should give a conservative estimate of limiting voltages. This curve may be used at any frequency, since the product of frequency and spacing is the controlling parameter.

The data applies to any connectors, transmission lines, or coaxial resonators which have no dielectric between the conductors.

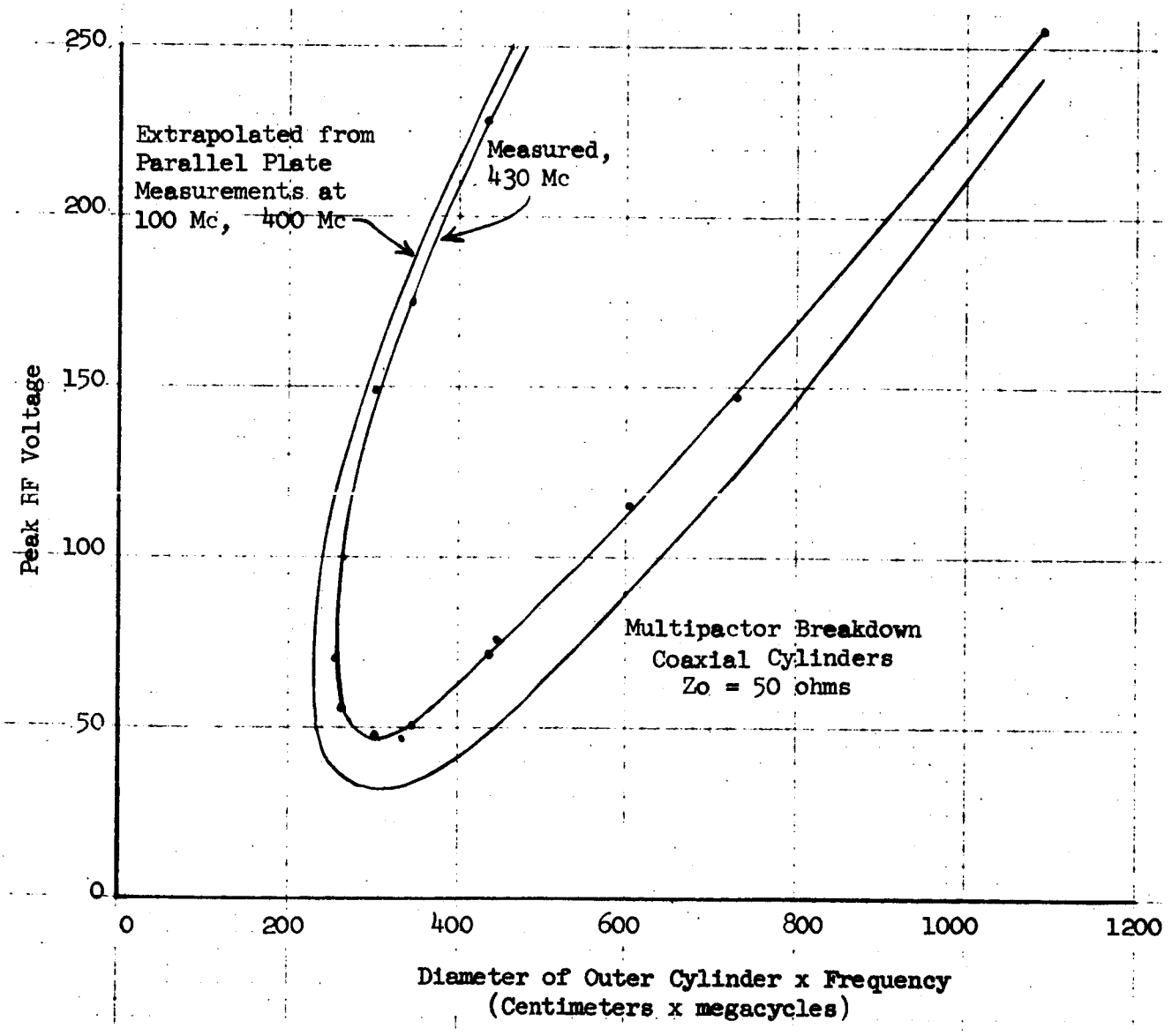

BREAKDOWN VOLTAGE versus SPACING

COAXIAL CYLINDERS 100 MC

Multipactor breakdown may exist inside the envelope of each curve.

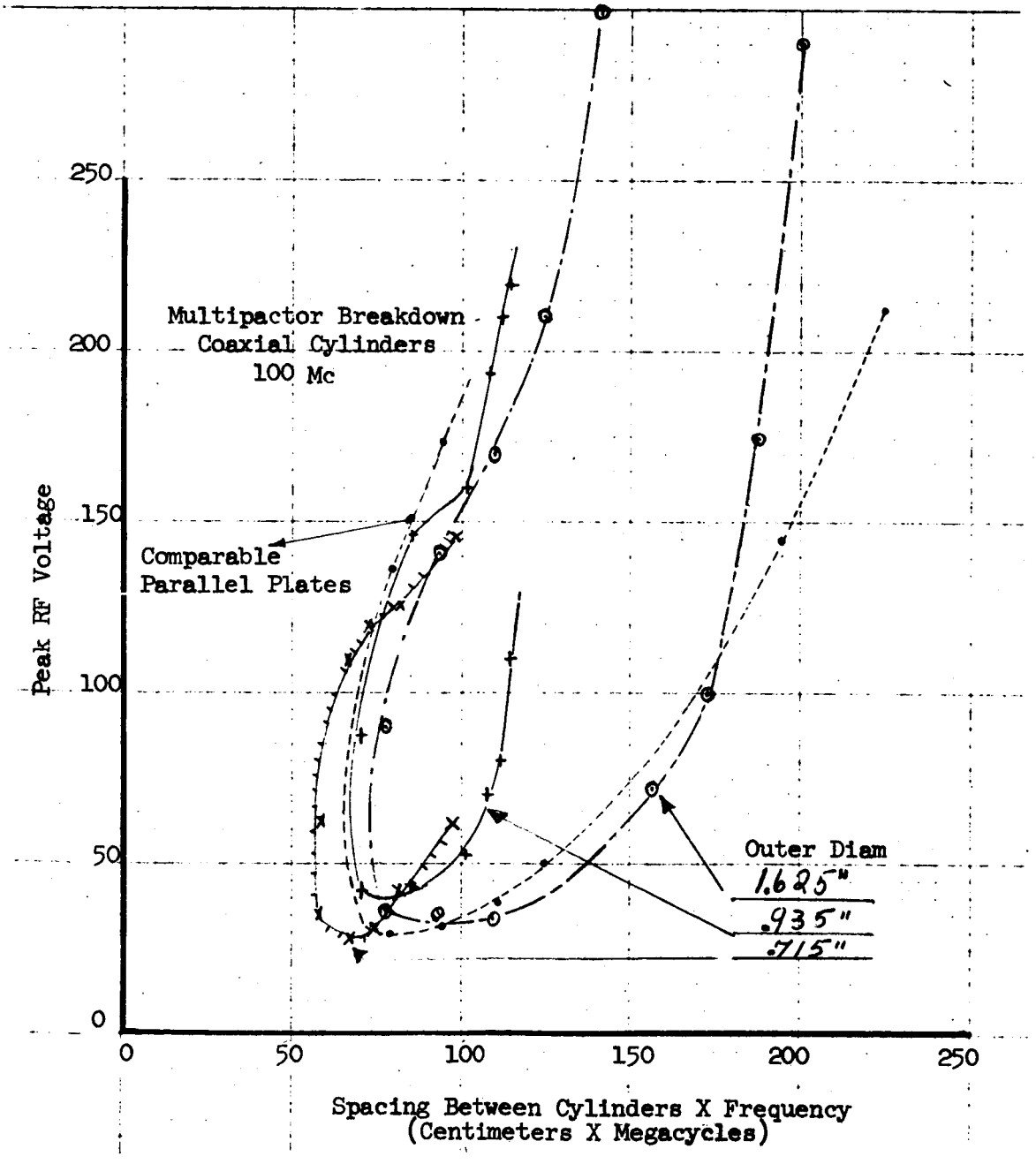

BREAKDOWN VOLTAGE versus SPACING COAXIAL CYLINDERS

430 megacycles

Breakdown exists inside the envelope of each curve.

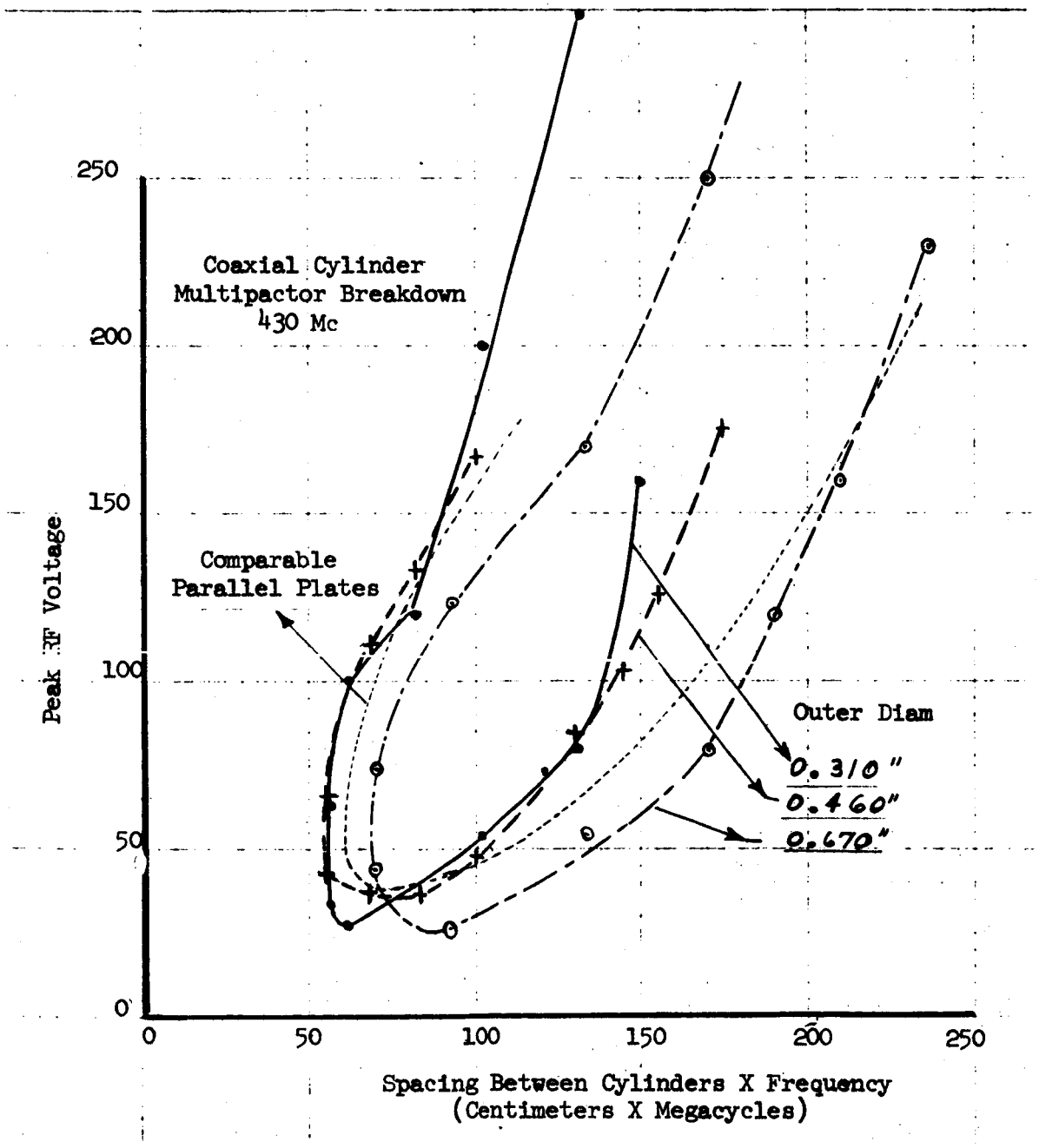

TYPICAL MULTIPACTOR CURRENT WAVEFORM

The waveform shown below was measured by means of a biased collector plate in the vacuum chamber. The relative amplitudes of the fundamental and harmonics are given in the equation printed on the chart. The test was performed at a frequency of 100 MHz between parallel plate electrodes.

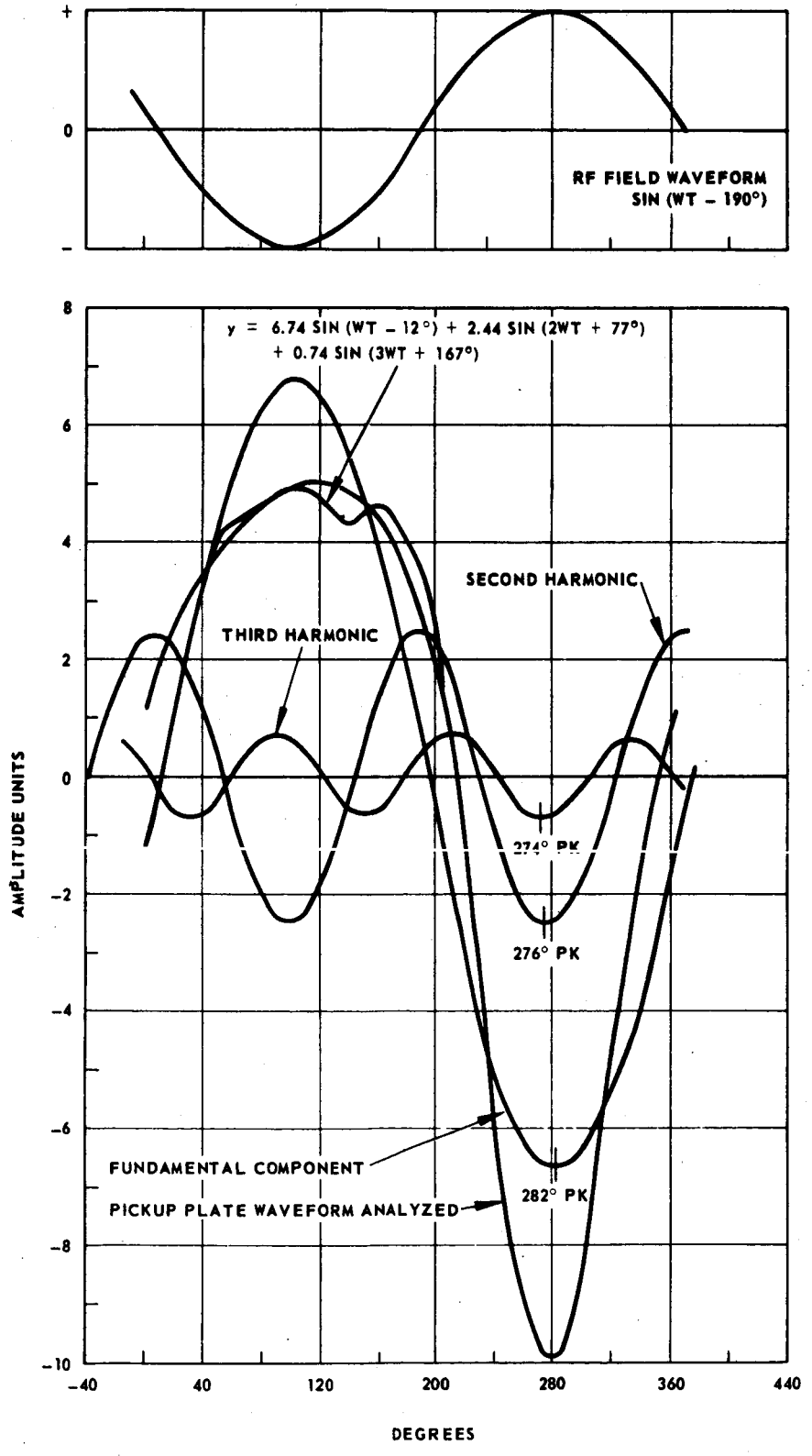

POWER LOSS IN MULTIPACTOR DISCHARGE
AS A FUNCTION OF PRODUCT f x d

This chart indicates the typical power density in milliwatts per sq. cm. for parallel plate multipactor at 100 MHz. The range of f x d which contains data is limited because of the voltage resonance condition necessary for a discharge; in brief, the power loss is nearly independent of f x d, when a discharge is possible.

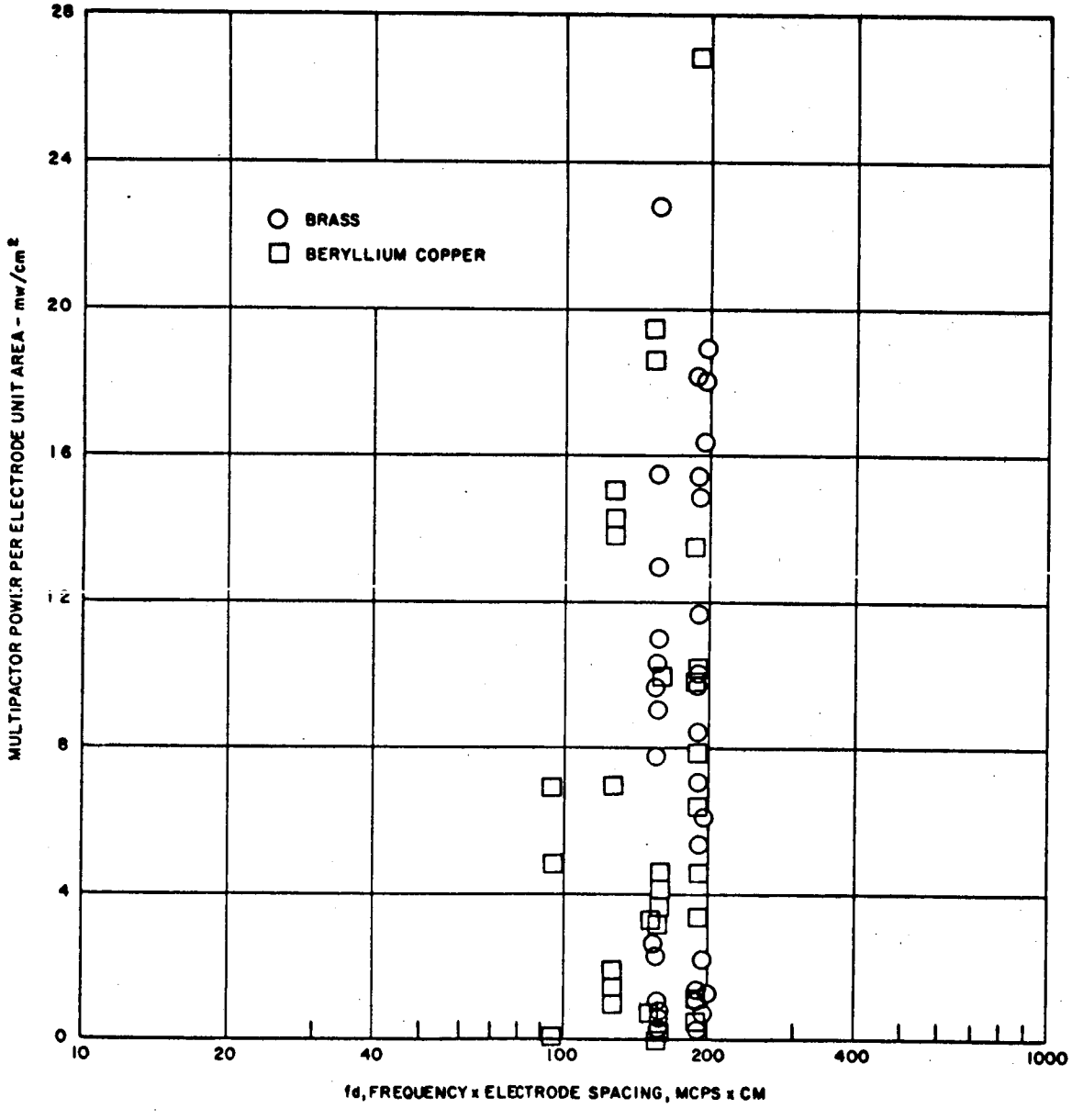

POWER LOSS IN MULTIPACTOR DISCHARGE
AS FUNCTION OF APPLIED VOLTAGE

The chart below summarizes measurements of power loss per unit area for common materials tested at frequencies of 100 MHZ and 430 MHZ, and may be used as an indication of the local heating effects.

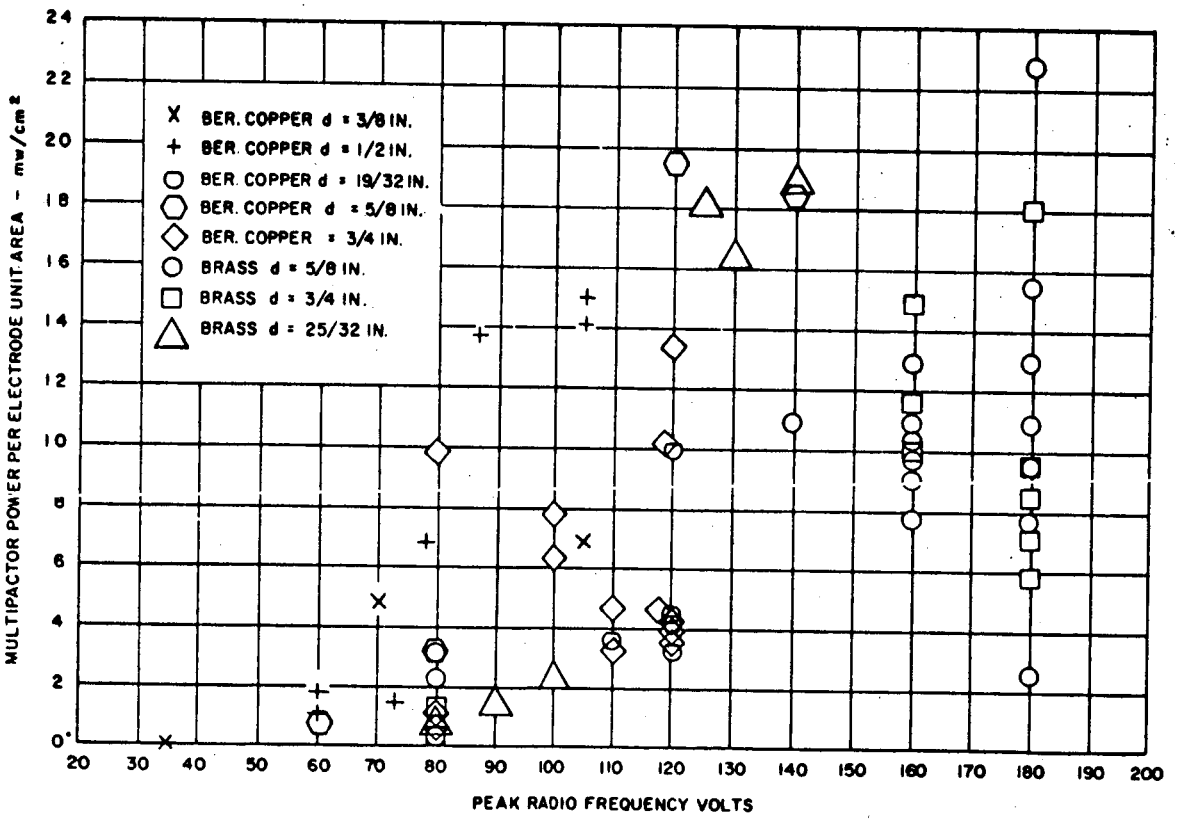

The single surface multipactor experiment was performed at 100 MHz with two values of spacing. The screen was treated carefully so as to eliminate the possibility of multipactor electron emission from it. Discharges were observed at RF voltage and d.c. bias values inside the envelope of the curves.

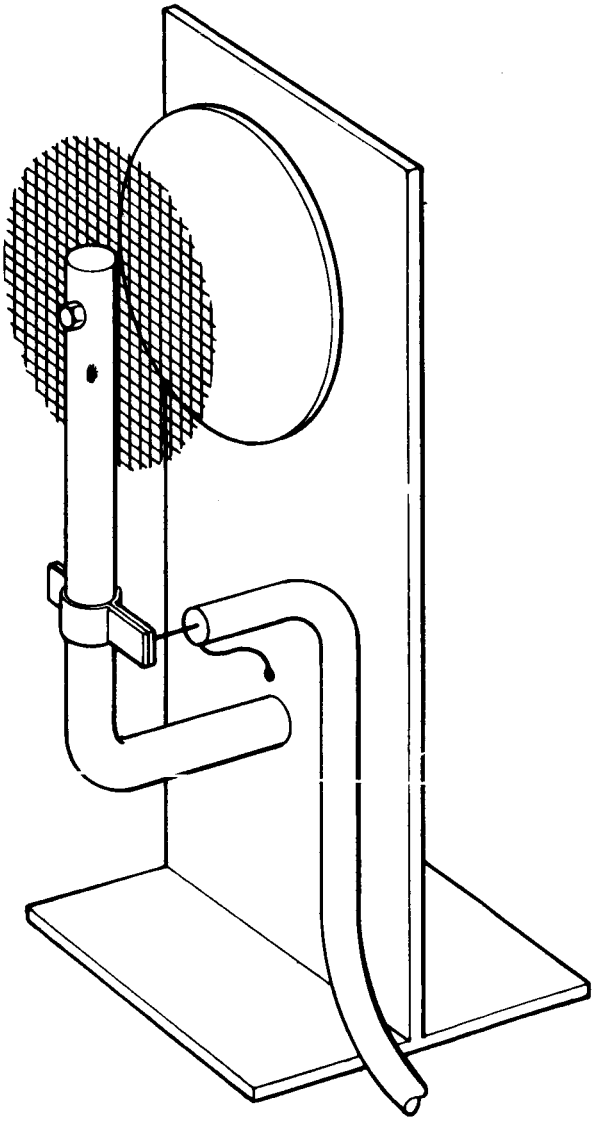

Single surface multipactor experiment

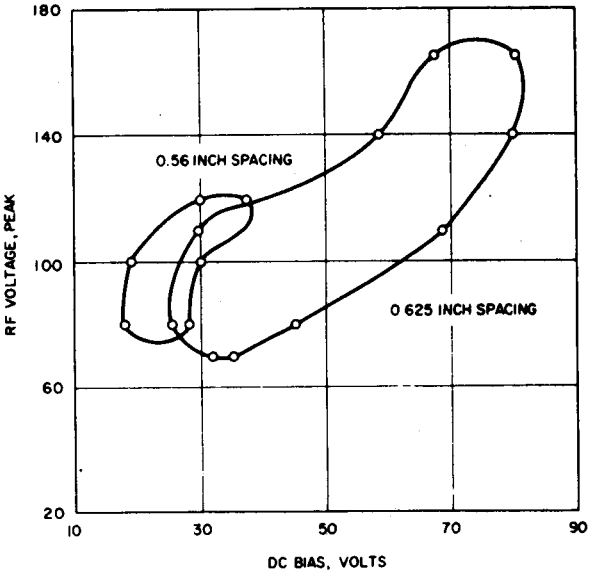

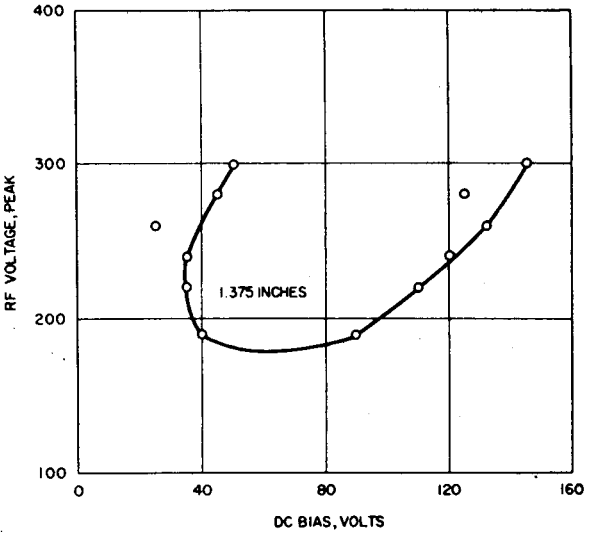

NOISE POWER IN MULTIPACTOR DISCHARGE

An experiment was performed to determine the noise power level produced 12 megacycles away from the frequency of the multipactor discharge. This spectrum separation corresponds to the NASA telemetry bands 136 MHz, 148 MHz, and the data is believed to be representative of the noise that would be generated by multipactor in such transmitters.

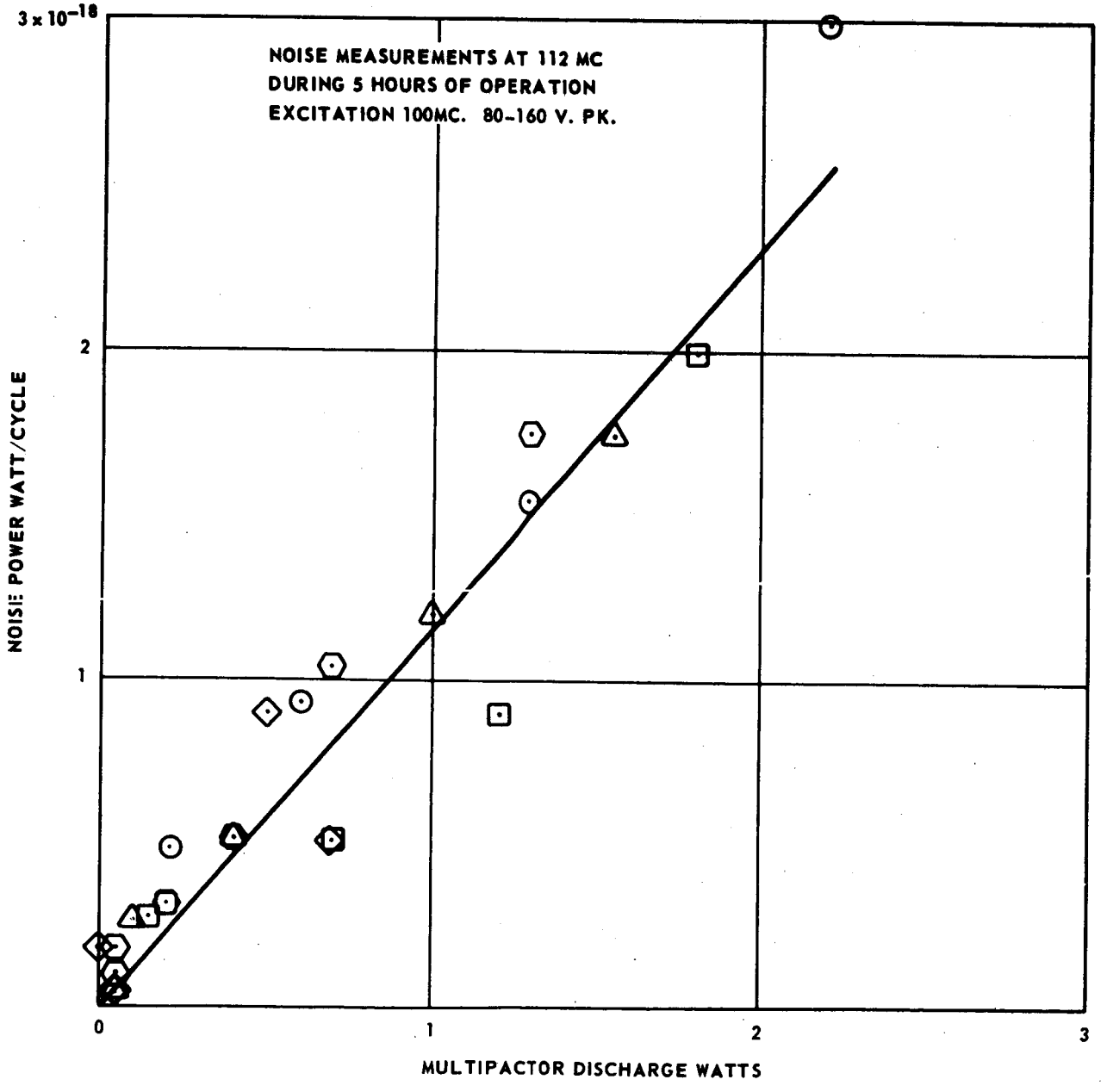

An experiment was performed to determine the level of noise power produced by a multipactor discharge at a frequency of 100 MHz. The noise was measured at several frequencies above and below the driving frequency. It seems clear that the noise power falls off with frequency separation as indicated by the lines for 118 MHz and 56.6 MHz.

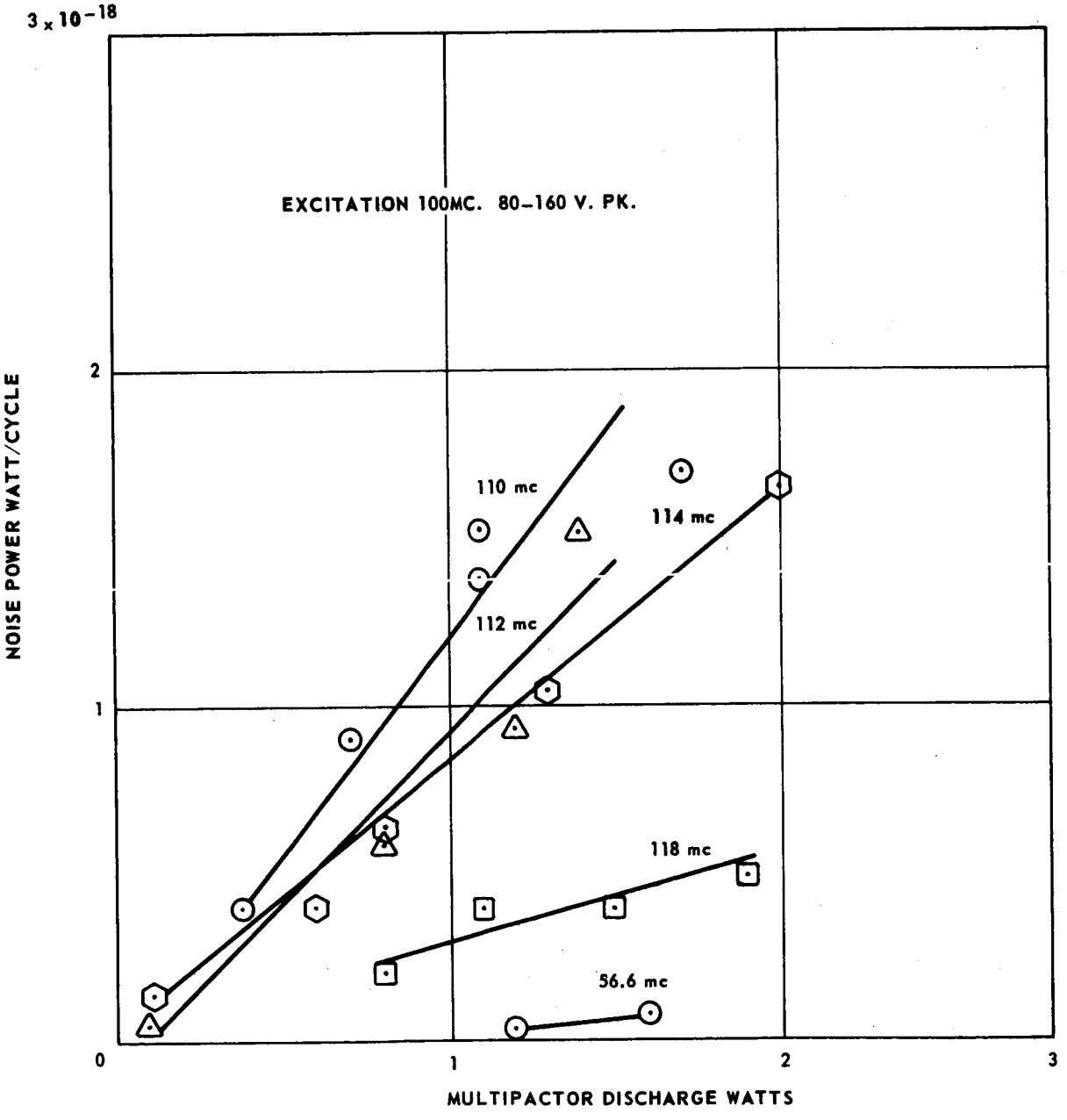

PRESSURE LEAKAGE versus TIME
For Crusted and Sanded Eccofoam

As noted in this handbook, the rate of leakage of outgassing products liberated by heating due to multipactor or other effects is a critical factor in determining the possibility of induced gas ionization breakdown. This curve indicates the relative leakage rates of identical foam samples 3/16" thick with surface crust in place or removed. It is obviously helpful to remove the crust, although it may not be sufficient to prevent a breakdown.

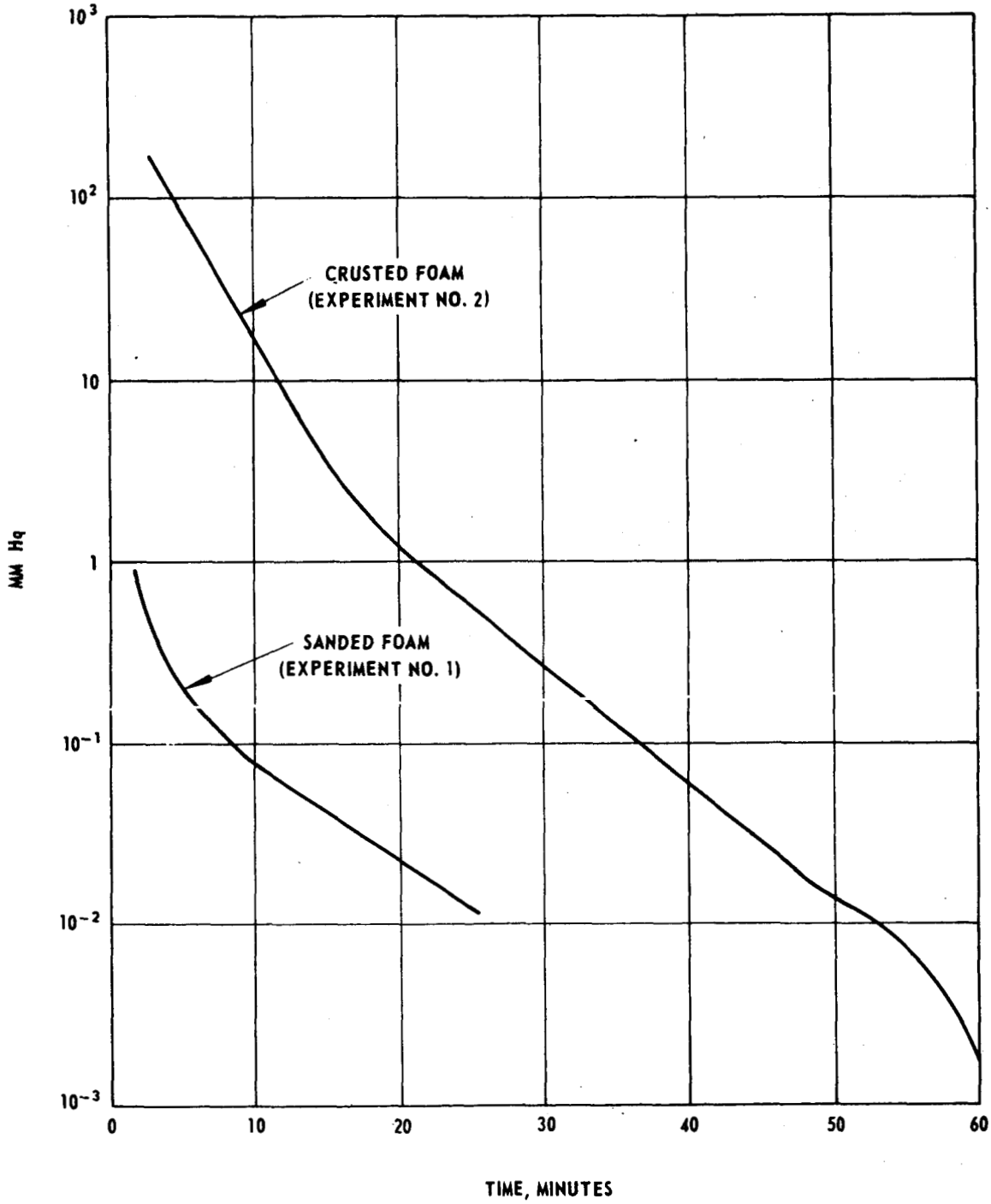

APPENDIX PART III

MULTIPACTOR THEORY

TABLE OF CONTENTS

INTRODUCTION

Secondary electron resonance breakdown or multipacting has been known and studied since 1924[13] and has been a matter of great concern to designers of high frequency vacuum tubes, including triodes, magnetrons, klystrons, and traveling wave tubes, as well as linear accelerators. It has been employed to practical advantage in the design of ultra-high speed microwave duplexers, switches[14], and cold cathode amplifiers[19]. Recently it has become a design problem in space electronics with the advent of high power transmitters that have component dimensions and frequencies that may be troubled by the effect. Both JPL[31] and Hughes Aircraft[4] have recently reported trouble with coaxial connectors and filters in transmitters designed for space applications. It has been suggested[52] that the sporadic transmission from the early Sputniks may have been due to multipacting breakdown in antennas and/or connectors.

This Appendix analyzes the resonance mechanism in plane and coaxial geometry with electric and/or magnetic fields for use in predicting the possibility of breakdown. Reference numbers refer to the Bibliography, Appendix Part IV.

TWO SURFACE MULTIPACTING

Multipacting between two surfaces is hypothesized to arise from a secondary electron resonance mechanism. According to this theory, a few electrons initially present are accelerated to an electrode where they produce secondary electrons. These secondary electrons are then emitted in a reversed electric field which carries them to another electrode surface in approximately one half cycle, producing another crop of secondaries which are in turn accelerated to the first surface, and so on. If the secondary emission yield is sufficiently greater than one, the number of oscillating electrons can be increased to a very large number in a short time. This large cloud of oscillating electrons causes sufficient ionization of the residual gas to result in breakdown of the gas.

Under optimum conditions, the electron is in phase with the field. Thus, an electron starting across the gap will collide with the walls and release secondary electrons just as the electric field passes through zero. The magnitude of the reversed electric field is such that the secondary electrons are accelerated back across the gap with a transit time that is equal to one half cycle.

It is obvious that a breakdown does not require the optimum conditions to occur, and there is a fairly broad region of fields and frequencies over which a phenomena may be observed. Breakdown is possible in a bounded region between two field values corresponding to too little or too much acceleration of the electrons to maintain the proper phase relations. As long as the electron mean free path and the r-f wavelength are both large compared to the electrode separation, the breakdown is independent of the

gas; although it is very dependent upon the electrode materials and surface conditions.

Parallel Plate Case:

Consider a chamber containing two parallel electrodes of separation d across which a voltage V sin wt is applied. Then an electron emitted with phase ϕ with respect to the field is acted on by the force

$$(1.1)\quad F = \frac{eV}{d}\sin(\omega t + \phi) = m\frac{d^2 z}{dt^2}$$

where the force F is directed along the z axis perpendicular to the electrodes.

Integrating, we get

$$(1.2)\quad \frac{dz}{dt} = \frac{eV}{m\omega d}\left[\cos\phi - \cos(\omega t+\phi)\right] + u_o$$

and

$$(1.3)\quad z(t) = \left[\frac{u_o}{\omega} + \frac{eV}{m\omega^2 d}\cos\phi\right]\omega t + \frac{eV}{m\omega^2 d}\left[\sin\phi - \sin(\omega t+\phi)\right]$$

where z (0) = 0 and U_o is the initial velocity of the electron along the z axis. Imposing the boundary condition that the transit time is an odd multiple of a half cycle, $z(t = n\pi/\omega) = d$, where n = 1, 3, 5, . . . , equations (1.2) and (1.3) yield:

$$(1.4)\quad u = \frac{2eV}{m\omega d}\cos\phi + u_o = \text{impact velocity}$$

$$(1.5)\quad d = \frac{\pi m u_o}{\omega} + \frac{eV}{m\omega^2 d}(n\pi\cos\phi + 2\sin\phi)$$

Solving for the voltage, in (1.5), we obtain:

$$(1.6)\quad V = \frac{m\omega^2 d^2}{e}\left[\frac{1 - \frac{\pi m u_o}{\omega d}}{\pi n\cos\phi + 2\sin\phi}\right]$$

By introducing Gill and von Engel's assumption that $k = U/U_o$ is the constant ratio of arrival velocity to emission velocity[16], equations (1.4) and (1.6) become:

$$(1.7)\quad \mathcal{U} = \left(\frac{k}{k-1}\right)\left(\frac{2eV}{m\omega d}\right)\cos\phi$$

and

$$(1.8)\quad V = \frac{m d^2 \omega^2}{e \Phi_n}$$

where

$$(1.9)\quad \Phi_n = \left(\frac{k+1}{k-1}\right)n\pi\cos\phi + 2\sin\phi$$

From equation (1.8), the breakdown strength can be minimized for fixed values of d and w by maximizing the value of Φ_n. Maximizing with respect to ϕ gives

$$(1.10)\quad \phi = \tan^{-1}\left[\frac{k-1}{k+1}\cdot\frac{2}{n\pi}\right]$$

If the value of k were known from fundamental considerations, then no further information would be needed to define most of the breakdown region. That is not the case however*, and the value of k has been found by semiempirical methods.

Hatch and Williams made extensive measurements of the breakdown potentials in such a way as to obtain both the maximum and minimum breakdown field strengths at various excitation frequencies.[28] Their data for the lowest order mode is shown in Figure 1. Data on the lower branch was taken by increasing the electric field strength until breakdown occurred. By suddenly applying a high field and then lowering it slowly, the upper breakdown curve was observed. It was found that a choice of $\Phi = 6.6$ provided a good fit to most of the data when using equation (1.8) with n = 1.

* Note the section on "Effects of Variations in Electron Energies"

Equations (1.8) and (1.9) then led to the empirically determined values $k = 3$ and $\phi = 18^{\circ}$. By assuming that k remained constant throughout the breakdown region, the upper breakdown curve was found to correspond to a value of $\phi = -56^{\circ}$. The results of this curve fitting are presented in Figure 2, and compared with the experimental curve in Figure 3.

Hatch extended the curve fitting to include the higher order modes, and his results are shown in Figure 4. The upper and lower bounds on the multipacting region arise from the condition that the electron arrival energy be such as to yield a secondary emission ratio greater than one. When this limitation is taken into account for the minimum arrival energy, it is found that, at a given spacing d, there is a minimum frequency f_{co} below which multipacting cannot occur. By combining equations (1.7) and (1.8), we find

$$(1.11) \quad f_{co} = \frac{(k-1)\,\Phi_u}{k\pi d \cos\phi_u}\left(\frac{e\,W_f}{8m}\right)^{1/2}$$

where W_f = minimum incident electron energy to yield a secondary electron emission ratio greater than one.

Φ_u = value of Φ on the upper portion of the breakdown region curve.

ϕ_u = value of ϕ on the upper portion of the breakdown curve.

which reduces to:

$$(1.12) \quad f_{co} = \frac{\text{constant}}{d}(W_f)^{1/2}$$

Figure 5 shown various measurements of cutoff frequency, compared to a calculated curve for $W_f = 40$ electron volts. Under these conditions, equation (1.12) reduces to:

$$(1.13) \quad f_{co} = \frac{79}{d}$$

where f_{co} is in megacycles and d in centimeters.[7]

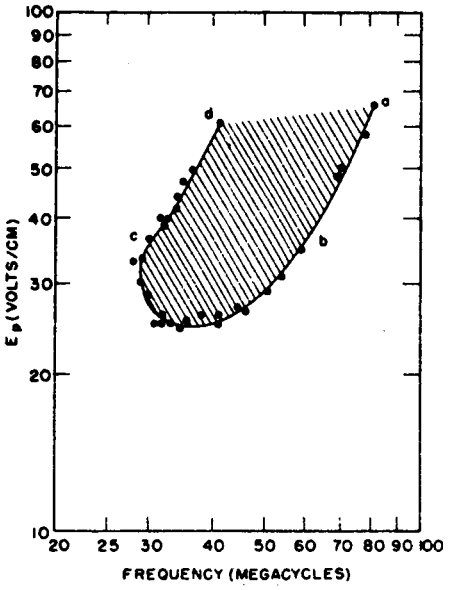

Figure 1. This graph shows the breakdown region (cross-hatched) in relation to the electric field strength and frequency observed with a gap spacing of 3 cm. in hydrogen at a pressure of less than 0.1 uHg. (From Hatch and Williams)

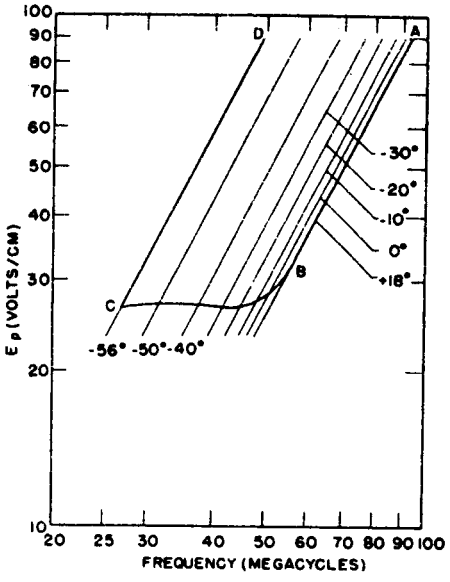

Figure 2. Theoretical calculation of breakdown region for 3 cm. separation, minimum electron arrival energy of 60 ev. and k = 3. Various lines represent condition for half cycle transit times at indicated phase angles. (From Hatch and Williams)

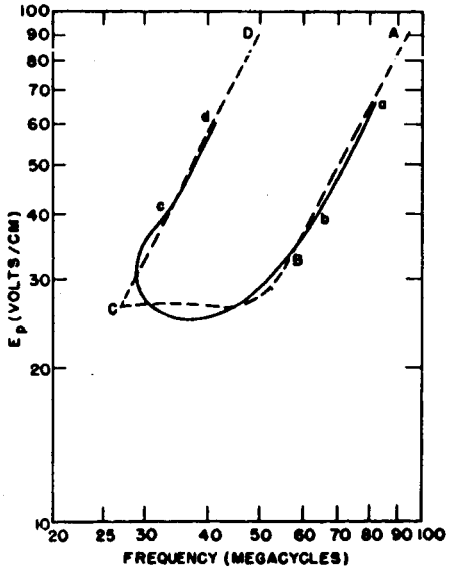

Area enclosed by solid line represents experimental region.

Area enclosed by dotted line represents theoretical region.

Figure 3. Comparison of experimental breakdown region of Figure 1 and theoretical breakdown region of Figure 2.

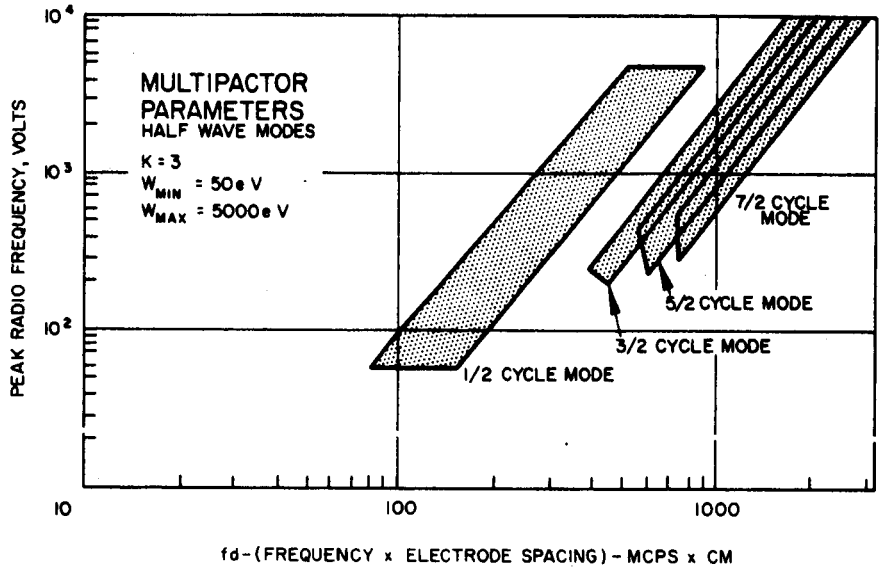

Figure 4. Possible Regions of Multipacting between Parallel Plates

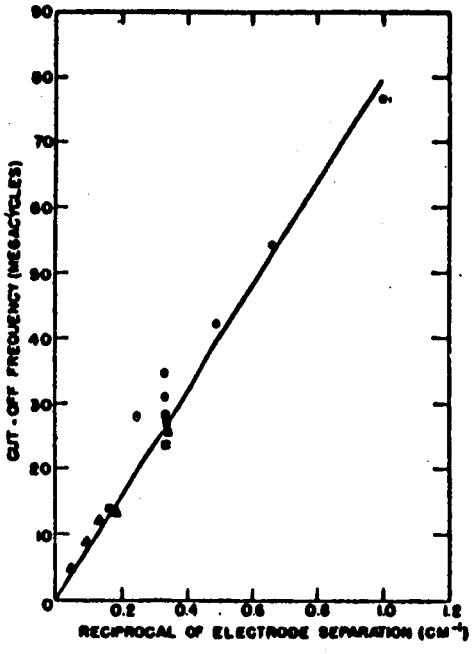

Fig. 5. Summary of cutoff frequencies versus reciprocal electrode separation from data of several observers.

▲ Gutton
■ Gill and von Engel
● Hatch and Williams
Solid line, cutoff law, $f_{co} = 79/L$

Parallel Plates with a D-C Bias

The effect of a bias voltage applied across a gap is to cause a difference in the transit times for incident and emitted electrons. By raising the bias enough to cause a significant difference in transit times, it is possible to prevent a stable multipacting discharge altogether. The analysis for this case has been worked out by the Sperry Gyroscope Company and C. Milazzo.

By assuming that the initial emission was zero, Sperry[48] was able to determine a definite cutoff bias for the various modes by considering the phase stability of the discharge. The conclusion reached as to the amount of bias needed to eliminate multipacting was as follows:

1/2 cycle transit time	$V_{dc} = 0.34\ V_1$
3/2 cycle transit time	$V_{dc} = 0.12\ V_1$
5/2 cycle transit time	$V_{dc} = 0.07\ V_1$

where $V_1 = \dfrac{\left(\dfrac{wd}{\quad}\right)^2}{\pi\left(\dfrac{e}{m}\right)^2}$

Other experimenters found multipacting phenomena for d-c. biases well in excess of those given by Sperry, and a more detailed treatment was made by Milazzo[40] in which the effects of finite emission velocities were taken into account. The results of his calculations are shown in Figure 6. However, experiments by Nance and Nanevicz[52] found breakdown occuring outside the region predicted by Milazzo as shown in Figure 7. It appears that this last phenomenon was due to a single surface multipacting mechanism (as described in the section on "Single Surface Multipacting: Parallel Electric Fields")that becomes possible when two surface multipacting can no longer occur.

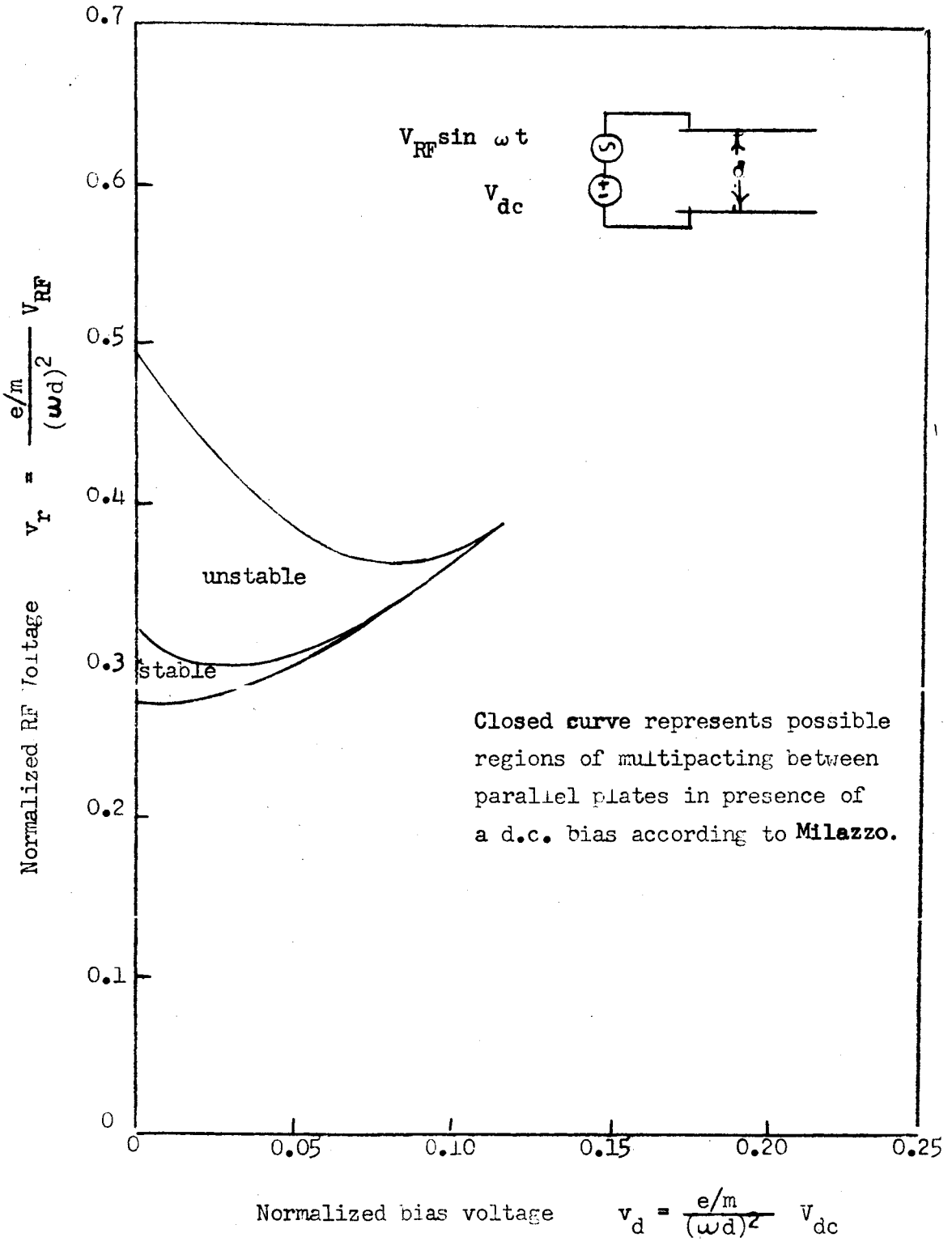

Figure 6. Theoretical Region of Multipacting With a D.C. Bias, after Milazzo

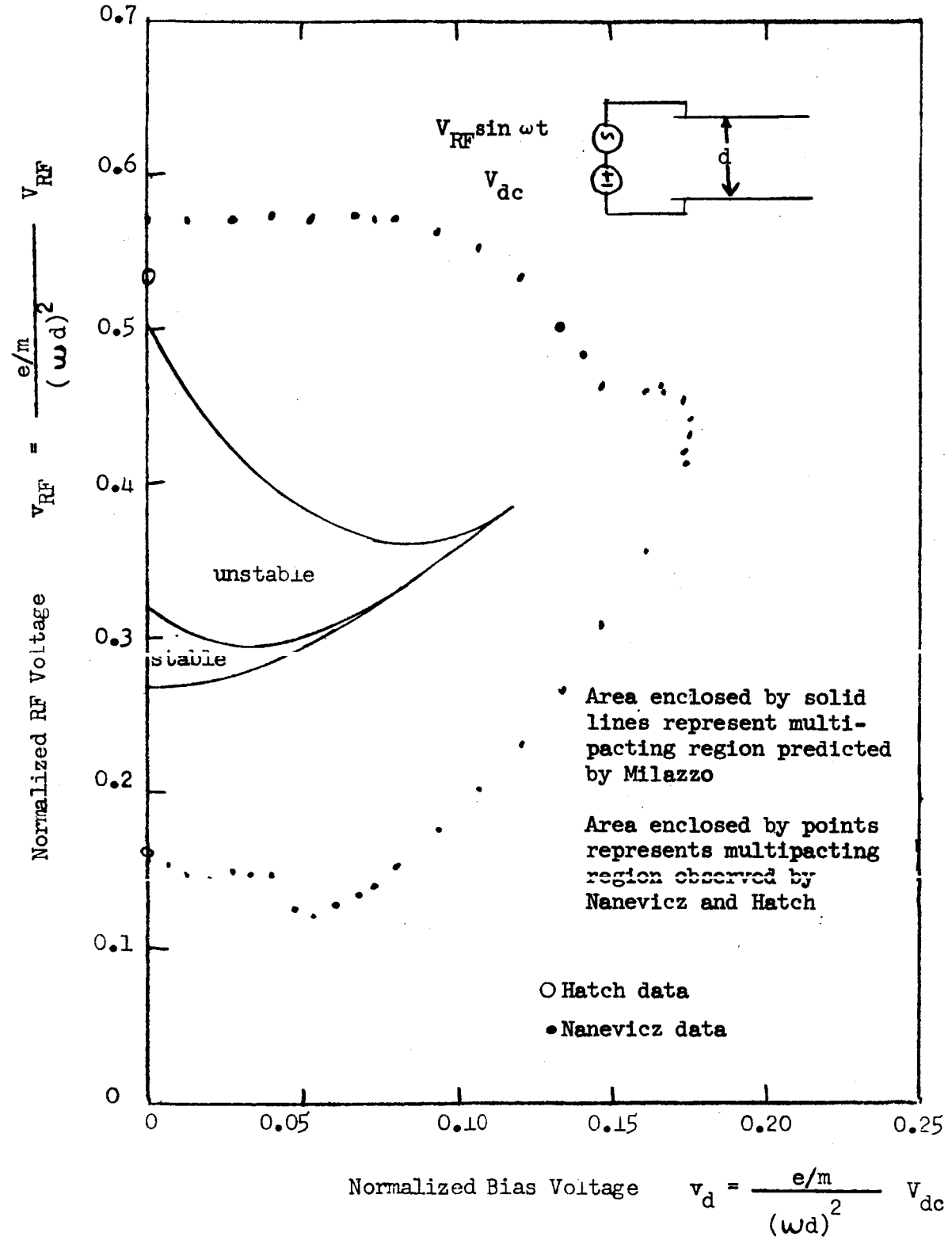

Figure 7. Theoretical and Experimental Regions of Biased Multipacting Discharge

after Vance and Nanevicz

Coaxial Cyclinders - No D-C Bias

The equation of motion for an electron moving between two coaxial cyclinders of radii a and b (a<b) with an r-f field V sin wt across the gap is:

$$(3.1)\quad m\frac{d^2r}{dt^2} = \frac{eV\sin(\omega t+\phi)}{r} = \frac{K\sin(\omega t+\phi)}{r}$$

Thus far, the nonlinear nature of this equation has prevented any closed form solution. Bol[5] attempted an approximate solution by studying a large number of trajectories with an analog computer. Only the lowest order mode was examined. The results are presented in Figure 8.

Unfortunately, Bol only considered the cases where the initial velocity was zero or one thousandth of the incident velocity, whereas it has been shown by several authors that setting the ratio of incident velocity to emission velocity at three gives much better agreement with experimental data. Since a lower value for this ratio allows multipacting over a larger region, Bol's results are useful only for very rough qualitative prediction; this conclusion is supported by the recent experimental results of Nanevicz[44] that have been plotted together with Bol's results in Figure 9. The large deviations from the theoretical predictions indicate that a more involved treatment of this configuration is needed.

Coaxial Cyclinders with a D-C Bias

As in the case of parallel plates with a d-c bias, a d-c bias between coaxial cyclinders reduces the possible regions of two surface multipacting by changing the transit time of the incident and emitted

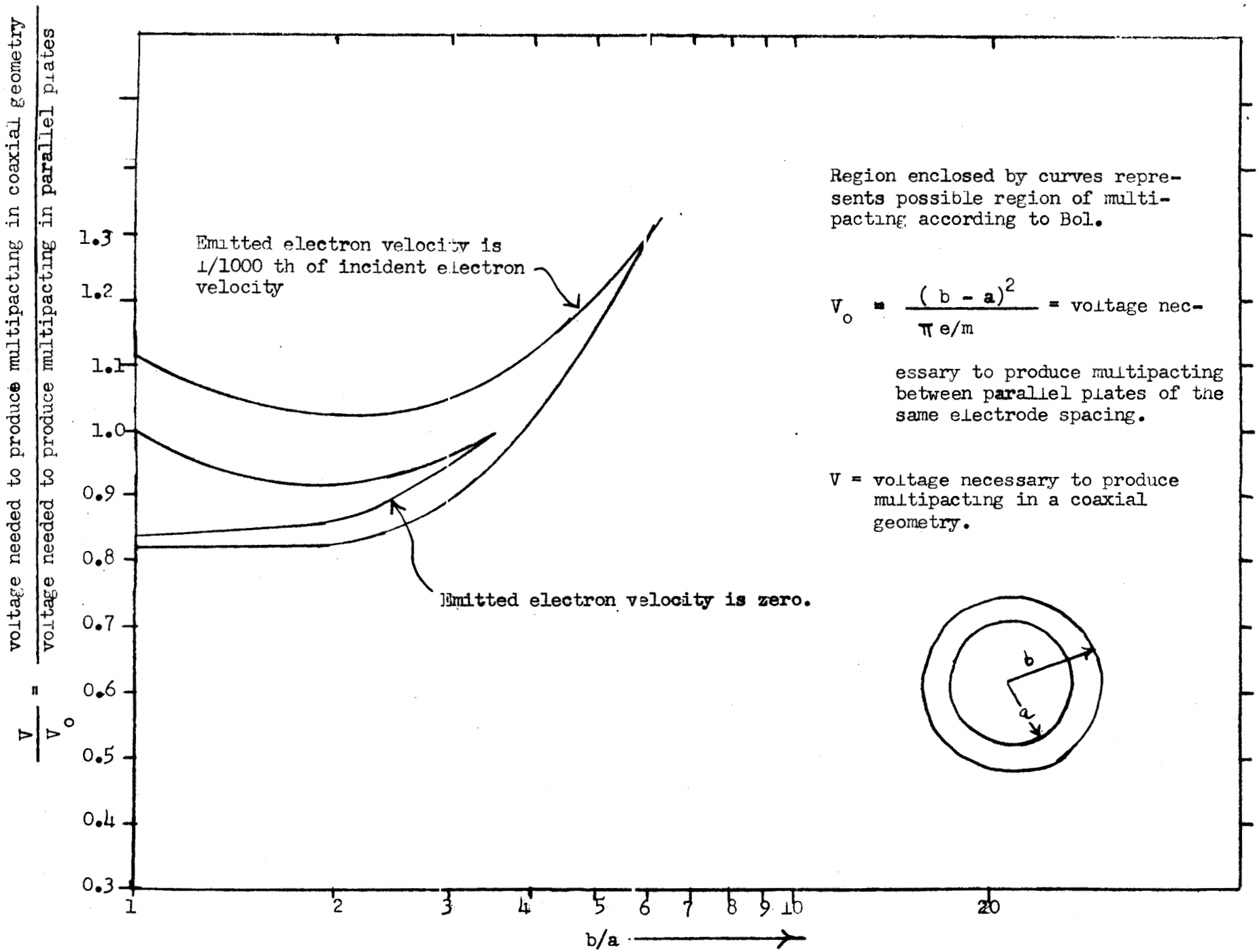

Figure 8. REGIONS OF MULTIPACTING BETWEEN COAXIAL CYCLINDERS, after Bol.

Figure 9. Calculated and Experimental Voltages for Multipacting in Coaxial Cyclinders

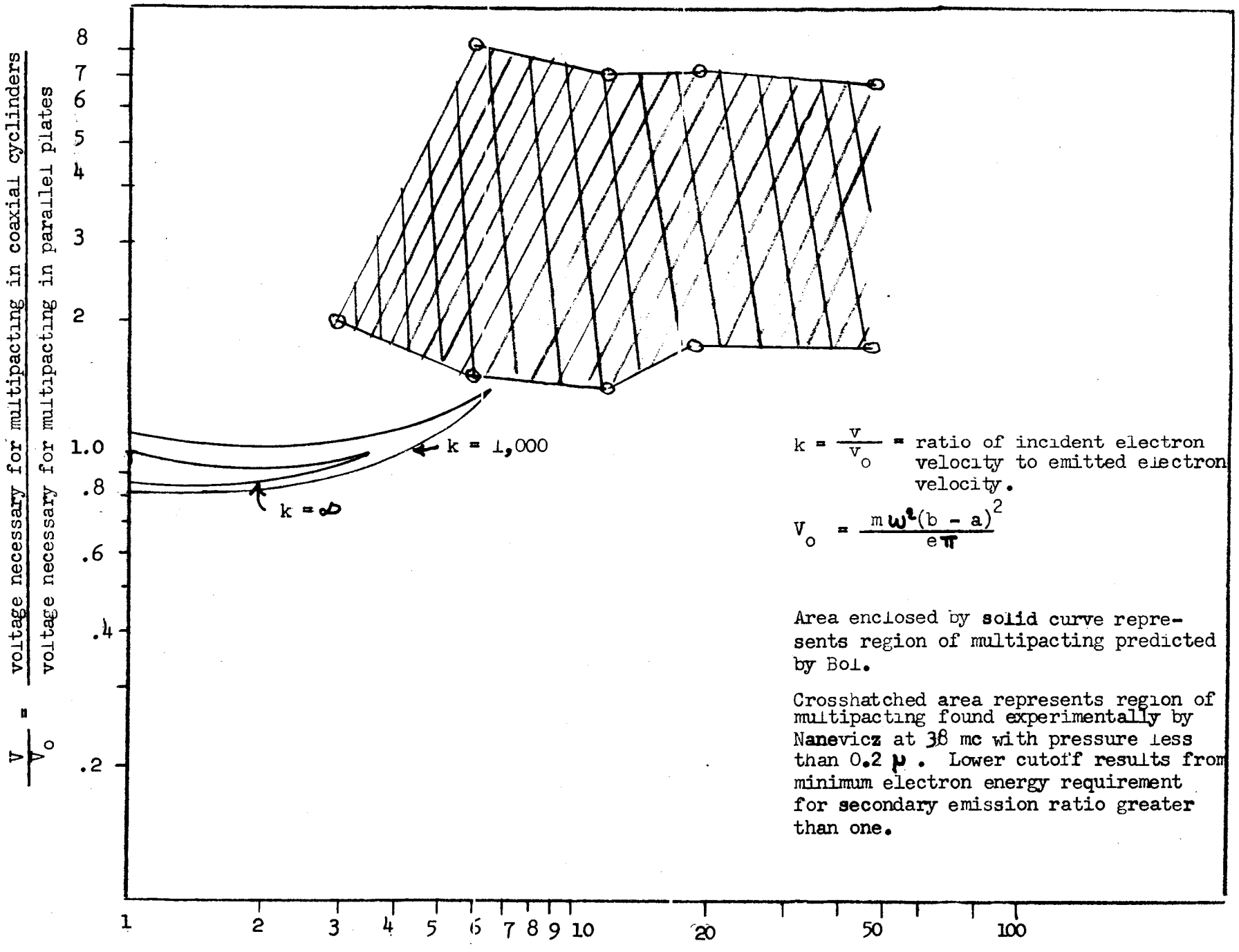

electrons. However, due to the nonlinear nature of the equations involved, no closed form or approximate solutions for this case have been made.

A further complicating factor is that a single surface multipacting mechanism can exist in the presence of a D-C. bias over a larger range of peak RF voltages than in the parallel plate case* (as is indicated by Nanevicz's results on the region of multipacting breakdown shown in Figure 10).

* E. Vance - personal communication.

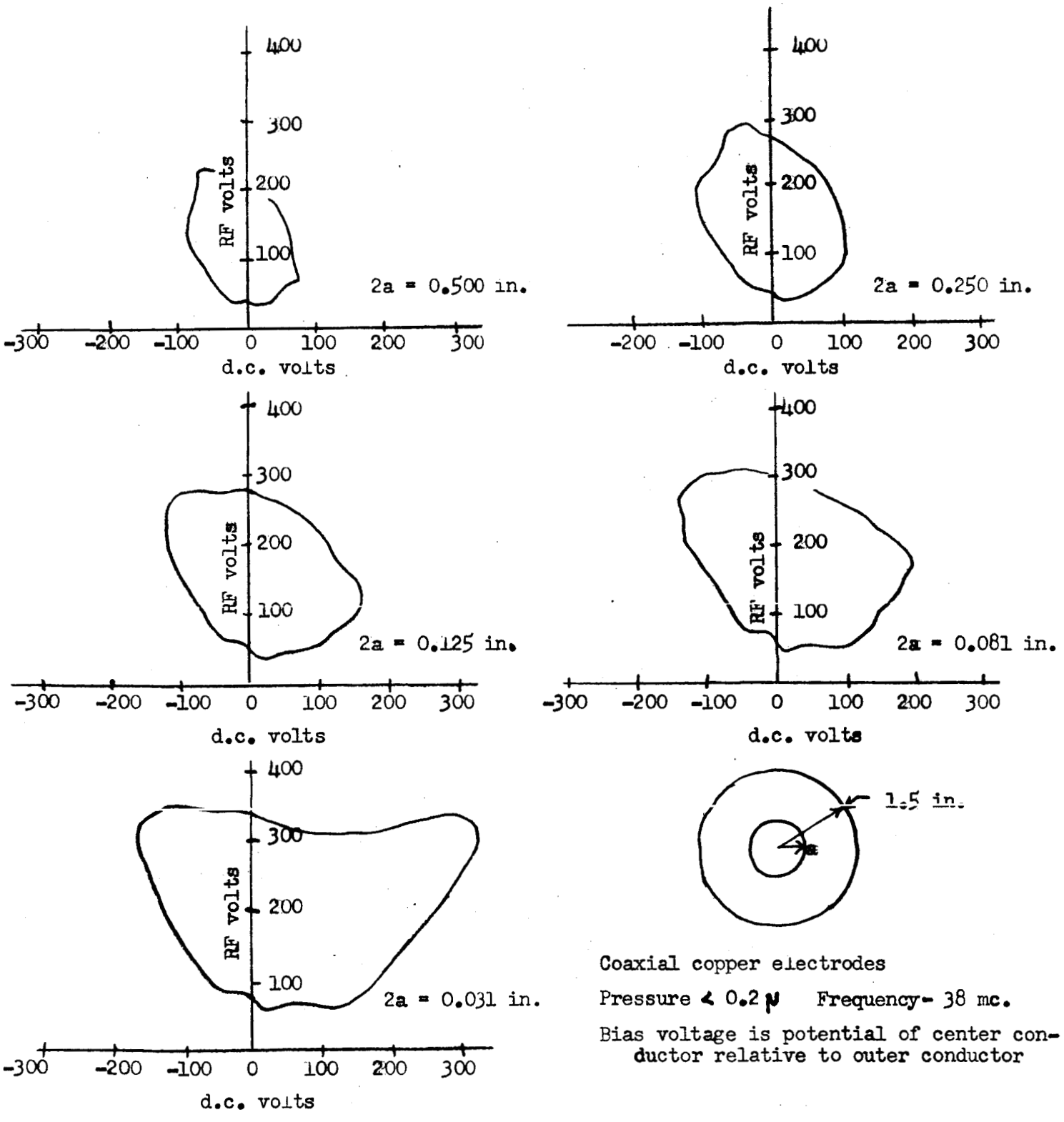

Coaxial copper electrodes

Pressure < 0.2 μ Frequency- 38 mc.

Bias voltage is potential of center conductor relative to outer conductor

Fig. 10 Regions of Multipacting Discharges in a Coaxial Geometry With D.C. Bias, after Nanevicz

SINGLE SURFACE MULTIPACTING - PARALLEL ELECTRIC FIELDS

The analysis of single surface multipacting in the presence of a d-c bias was first made by Vance and Nanevicz[52] when they obtained multipacting over a much wider range of voltages than predicted by the theory of either Bol[5] or Milazzo[40]. A typical example of this was shown in Figure 9.

In the analysis of single surface multipacting, the usual assumptions of negligible space charge and mean free path much greater than gap spacing are made so that the instantaneous electric field in the gap d between parallel plates is

$$(5.1)\quad E(t) = \frac{V_{DC}}{d} + \frac{V_{RF}}{d}\sin\omega t .$$

The acceleration of an electron will be of the form

$$(5.2)\quad \frac{d^2x}{dt^2} = \frac{eV_{DC}}{md}(1+\alpha\sin\omega t)$$

where $\alpha = V_{rf}/V_{dc}$ is the ratio of peak RF voltage to the dc voltage. Integrating, we obtain

$$(5.3)\quad \text{electron velocity} = \frac{dx}{dt} = u_0 + \frac{eV_{DC}}{m\omega d}\left[\phi_0 - \omega t + \alpha(\cos\omega t - \cos\phi)\right]$$

and

$$(5.4)\quad \frac{x}{d} = \frac{u_0}{\omega d}(\omega t - \phi_0) + \frac{eV_{DC}}{\omega^2 m d}\left[-\frac{(\omega t-\phi_0)^2}{2} + \alpha\left\{\sin\omega t - \sin\phi_0 - (\omega t-\phi_0)\cos\phi_0\right\}\right]$$

where it has been assumed that the electron is emitted at wt = ϕ_o with an initial velocity u_o and zero initial displacement.

The boundary conditions that determine the region over which multipacting is possible are:

1. The electron emitted at wt = ϕ_o must return to the electrode at the end of the r-f cycle with sufficient energy to yield a secondary emission ratio greater than one.
2. The maximum displacement cannot exceed tha gap spacing d unless the electron be lost to the opposite electrode, and the minimum displacement for $\phi_o \leq$ wt $\leq \phi_o + 2\pi$ must be greater than zero after emission if the electron is to remain free of the electrode.

If u_1 is the magnitude of the velocity when the electron has the required impact energy, we obtain from Eq. (5.3) evaluated at wt - $\phi_o = 2\pi$ the condition

$$(5.5)\quad \frac{dx}{dt} = u_o - 2\pi \frac{eV_{DC}}{m\omega d} \leq -u_1$$

Defining the normalized bias voltage $v_d = \frac{e/m}{\omega^2 d^2}$ Vdc, this becomes

$$(5.6)\quad V_d \leq \frac{k+1}{2\pi\theta}$$

where $\theta = \frac{\omega d}{u_o}$ and, following Gill and von Engel, $k = \frac{u_1}{u_o}$. Applying the condition that the electron returns to the emitting electrode at the end of one r-f cycle to equation (5.4) gives

$$(5.7)\quad V_d = \frac{1}{\theta(\pi + \alpha\cos\phi)}$$

Thus, for a given frequency, gap width and r-f voltage, single surface multipacting cannot occur unless the dc bias voltage defined by Eq. (5.7) exceeds the minimum value defined by equation (5.6).

Applying the second boundary condition to equations (5.3) and (5.4) gives the requirements:

$$(5.8)\quad V_d = \frac{\phi_1 - \phi_0}{\theta\,\frac{(\phi_1-\phi_2)^2}{2} - \alpha\theta\left[\sin\phi_1 - \sin\phi_0 - (\phi_1-\phi_0)\cos\phi_0\right]}$$

and

$$(5.9)\quad 1 > \frac{\phi_2-\phi_1}{\theta} + V_d\left\{-\frac{(\phi_2-\phi_0)^2}{2} + \alpha\left[\sin\phi_2 - \sin\phi_0 + (\phi_2-\phi_0)\cos\phi_0\right]\right\}$$

where $wt = \phi_1$ = phase at which x is minimum

$wt = \phi_2$ = phase at which x is maximum

Using a graphical technique, Vance was able to eliminate θV_d between Eqs. (5.6) and (5.8) to obtain α as a function of ϕ_0 for the minimum displacement. When phase stability is also taken into account, the lower threshold of RF voltages is given by:

$$(5.10)\quad \frac{eV_{RF}}{m(\omega d)^2} = \alpha V_d = \pi\left(V_d - \frac{1}{\theta\pi}\right)$$

Figure 11 shows how these various requirements yield a region for which stable multipacting is possible.

When we also take into account higher order modes and the region in which two surface multipactor is possible as given by Milazzo[40], we obtain Figure 12 from which it is possible to predict whether a given gap spacing, bias, r-f voltage and frequency will yield multipacting in the parallel plate geometry.

For comparison, the regions of experimentally observed multipactor discharge are plotted together with the theoretical region in Figure 13. Vance[52] attributes the differences to be due mainly to the idealizations of the theory in which the finite thickness of the electron cloud, the effect of oxide films and other contaminants and the distribution of emission energies are not taken into account.

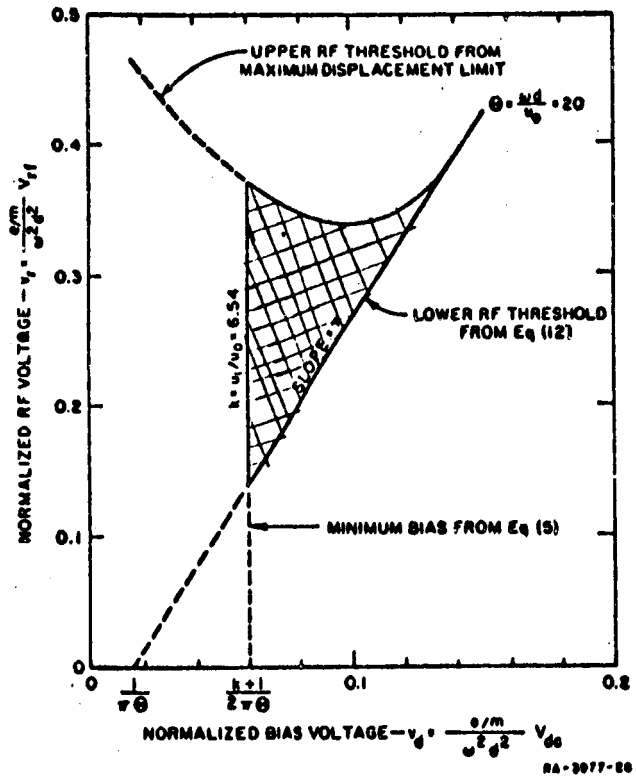

Figure 11. This figure illustrates how the upper and lower RF thresholds and minimum d.c. bias combine to yield the crosshatched region where one sided multipacting discharge is possible.
(after Vance and Nanevicz)

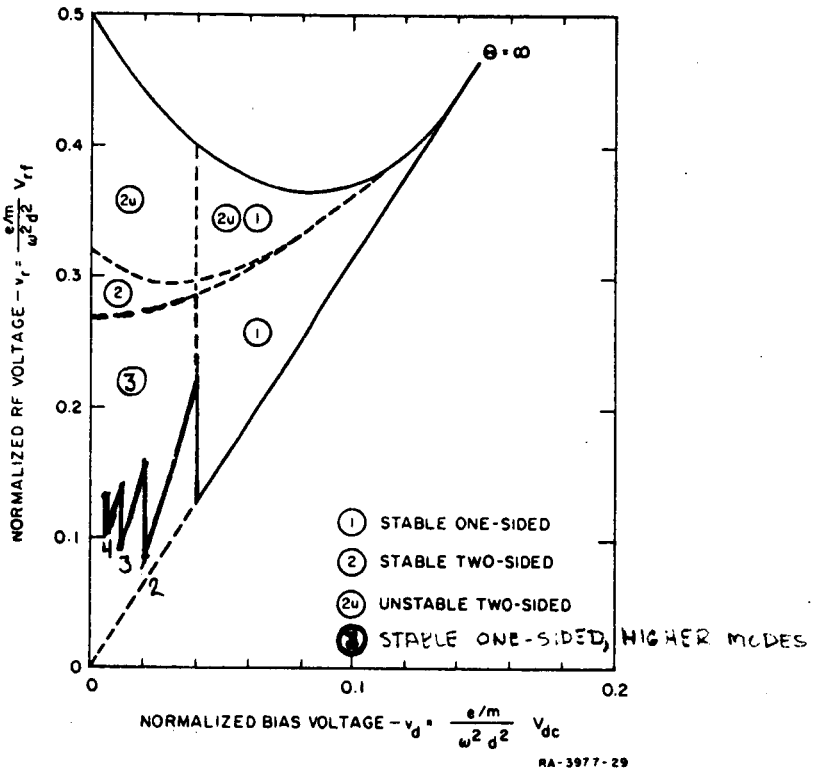

Figure 12. Biased Multipactor Discharge Region Including One-Sided and Two-Sided Modes

This figure illustrates how a multipacting discharge may be possible over a considerable range of RF voltages and d.c. biases due to the various modes of discharge that can exist. The numbers at the lower bound of the region of "one-sided multipacting, higher modes" represent the number of RF cycles involved in one electron cycle for the various modes.

after Vance and Nanevicz.

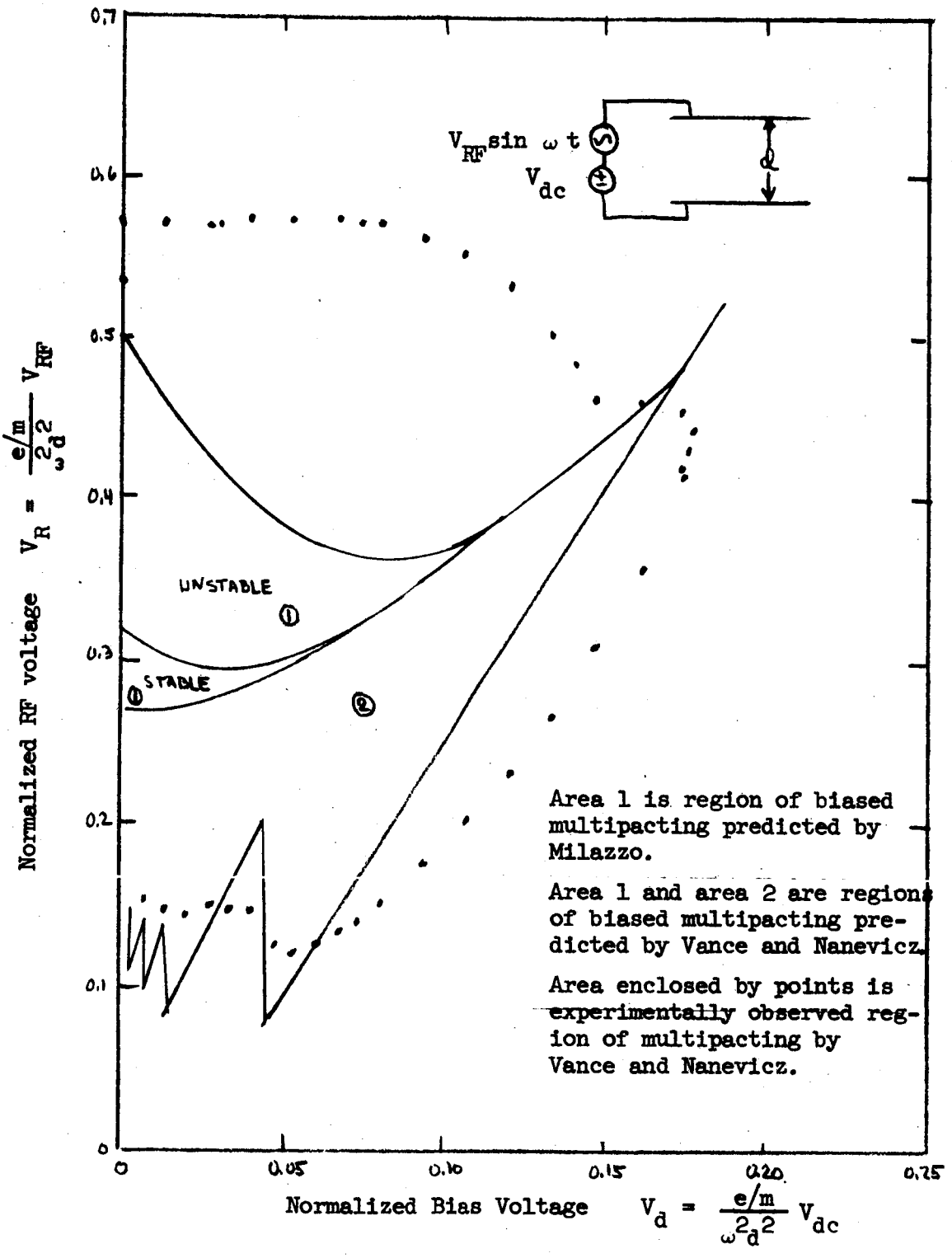

Figure 13. Theoretical and Experimental Regions of Biased Multipactor Discharge, after Vance and Nanevicz

Single-Surface Multipacting with Mutally Perpendicular Electric Fields:

Multipacting on a single surface in the presence of a mainly tangential r-f field and a small bombarding stream of electrons having velocities in the range that lead to a secondary emission ratio greater than one was first observed by Preist [45] as it caused the heating of output windows in klystrons. The discussion and analysis presented here are his.

When an initial stream of electrons is incident on a surface with enough energy to release secondary electrons, the electrons will, in the absence of any other force upon them, travel away from the surface as shown by path 1 in Figure 14. If there is a constant force tending to return the electrons to the surface, their trajectories will be as shown by dotted paths 2 and 3, the distance traveled before return depending on the relative values of F, U_o and Ep. F and Ep are electric field strengths defined in Figure 14.

If the arrival velocity of the secondaries is high enough to liberate more than one secondary, there can be a rapid multiplication of the secondaries present with a consequent build-up of dissipation. Since the velocity of the secondary is a periodic function of time due to the acceleration of the periodic field, the kinetic energy is also a periodic function of time. There are, therefore, many possible arrival times one r-f period apart which will allow the maximum kinetic energy to be given to the electron. It can be inferred that there is a wide range of values of Ep, U_o and F which will permit multiplication to occur.

The equations of motion for an electron above the surface shown in Figure 14C are:

$$(6.1)\quad \frac{d^2x}{dt^2} = \frac{e}{m}\left[E_{RF}\sin \omega t\right]$$

$$(6.2)\quad \frac{d^2y}{dt^2} = -\frac{e}{m}E_{DC}$$

where E_{RF} is the alternating electric field parallel to the surface and E_{DC} is a static electric field normal to the surface.

Integrating, we obtain

$$(6.3)\quad \frac{dx}{dt} = -\frac{e E_{RF}}{m}\left[\cos\omega t - \cos\omega t_o\right] + u_{ox}$$

$$(6.4)\quad \frac{dy}{dt} = -\frac{e E_{DC}}{m}(t - t_o) + u_{oy}$$

and

$$(6.5)\quad x(t) = -\frac{e E_{RF}}{m\omega^2}\left[\sin\omega t - \sin\omega t_o\right] + \frac{e E_{RF}}{m\omega^2}(\cos\omega t_o)(\omega t - \omega t_o) + u_{ox}(t - t_o)$$

$$(6.6)\quad y(t) = -\frac{e E_{DC}}{2m}(t - t_o)^2 + u_{oy}(t - t_o)$$

where the electrons leave the point $x = y = 0$ at $t = t_o$ with initial velocity $\vec{u} = u_{ox}\vec{a}_x + u_{oy}\vec{a}_y + u_{oz}\vec{a}_z$. The maximum velocity in the x direction occurs when $\omega t = (2n + 1)\pi$, and $\omega t_o = 2n\pi$ where n is an integer.

$$(6.7)\quad u_{x\,max} = 2\frac{e}{m}\frac{E_{RF}}{\omega} + u_{ox}$$

The average impact kinetic energy of these secondary electrons striking at $\omega t = \pi(2n + 1)$ is

$$(6.8)\quad E = \tfrac{1}{2} m \overline{u_x^2 + u_y^2 + u_z^2}$$

where the average is over the statistical distribution of the electrons in various direction with various velocities. Since:

$$\overline{u_{x\,impact}^2} = \overline{\left[2\left(\frac{e E_{RF}}{m\omega}\right)\right]^2} + \overline{4\frac{e E_{RF}}{m\omega}u_{ox}} + \overline{u_{ox}^2}$$

$$= \left(2\frac{e E_{RF}}{m\omega}\right)^2 + \overline{u_{ox}^2}$$

$$\overline{u_{y\,impact}^2} = \overline{u_{oy}^2}$$

$$\overline{u_{z\,impact}^2} = \overline{u_{oz}^2}$$

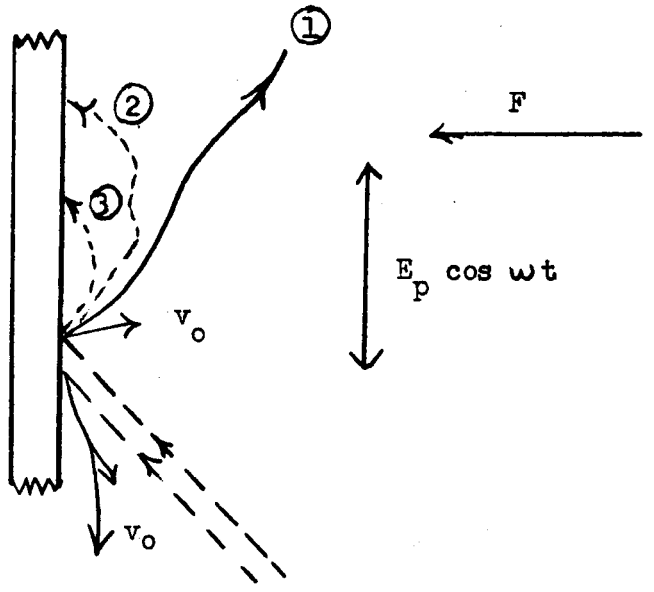

Figure 14. Typical Electron Motions in Perpendicular Electric Fields, after Priest

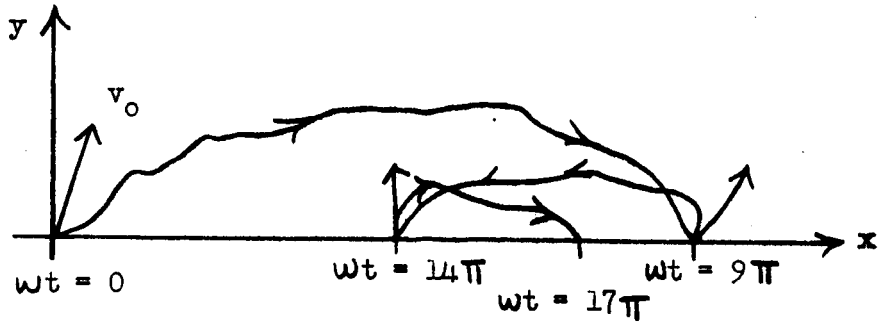

Examples of Electron Trajectories

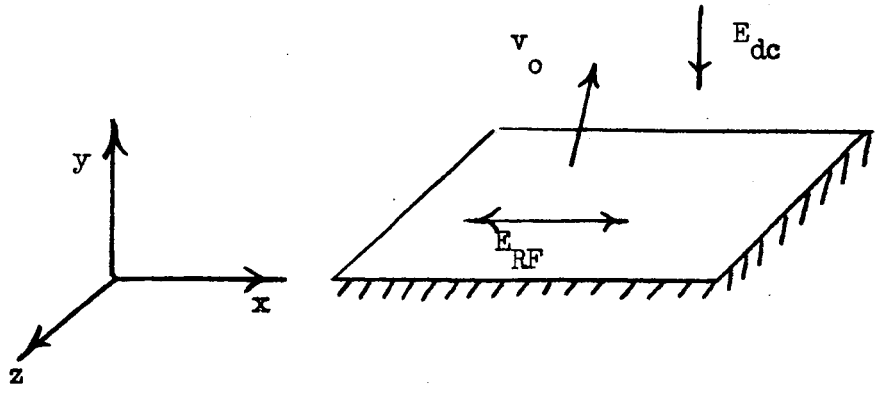

Field and Velocity Orientations in Single Surface Multipacting With Mutually Perpendicular Electric Fields, after Priest

and the initial electron energy is:

$$(6.9)\quad eV_0 = \frac{1}{2} m \left(u_{0x}^2 + u_{0y}^2 + u_{0z}^2\right)$$

we get:

$$(6.10)\quad E = \frac{2e^2}{m}\left(\frac{E_{RF}}{\omega}\right)^2 + eV_0 = eV = \frac{1}{2} m u_{impact}^2$$

Or, in terms of $k = \frac{u_{impact}}{u_0}$, we have

$$(6.11)\quad V = 2\left(\frac{e}{m}\right)\left(\frac{E_{RF}}{\omega}\right)^2\left(\frac{k^2}{k^2-1}\right)$$

The criterion for multipacting then becomes:

1. $\frac{2e}{m}\left(\frac{E_{RF}}{\omega}\right)^2\left(\frac{k^2}{k^2-1}\right) \geq V_{min}$

   where V_{MIN} is the minimum potential necessary to produce a secondary electron emission ratio greater than one.

2. The incident electrons from the bombarding stream must have a high enough incident energy to yield a secondary emission ratio of one.

The constant electric force may be maintained by space-charge potential gradients, especially in the case of dense electron beams, so that an external bias might not be necessary to yield breakdown.

Single Surface Multipacting in a Magnetic Field

In a magnetic field strong enough to bend the path of the electron and to return it to its surface of origin, it is possible to have a secondary electron resonance.

There are two special cases of interest, one in which the electric and magnetic fields are mutually perpendicular, the other when they are parallel. The first case has been studied by several authors and thoroughly analyzed by Brown[17]. The analysis presented here will follow Brown's treatment.

The equation of motion for an electron in an electric field $\vec{E} = \vec{a_x} E_0 \cos(\omega t + \phi)$ directed normal to the wall located at x = 0 and a static magnetic field $\bar{B} = \bar{a}_z B_0$ directed parallel to the wall is

$$(7.1)\quad m \frac{d\vec{v}}{dt} = -e(\vec{E} + \vec{v} \times \vec{B})$$

From Equation 7.1 the kinetic energy of the electron can be obtained as

$$(7.2)\quad W = \frac{1}{2} m |v|^2 = \frac{e^2 E_0^2}{2m} \left\{ \frac{\sin^2 [\frac{1}{2}(\omega+\omega_b)t]}{(\omega+\omega_b)^2} + \right.$$

$$\left. \frac{\sin^2 [\frac{1}{2}(\omega-\omega_b)t]}{(\omega-\omega_b)^2} + \frac{2\cos(\omega t+\phi)\sin\frac{1}{2}(\omega+\omega_b)t \sin\frac{1}{2}(\omega-\omega_b)t}{(\omega+\omega_b)(\omega-\omega_b)} \right.$$

as well as the electron position along the x axis

$$(7.3)\quad x = \frac{e E_0}{2m} \left[\frac{\cos(\omega t+\phi)}{\omega(\omega+\omega_b)} + \frac{\cos(\omega_b t-\phi)}{\omega_b(\omega_b+\omega)} + \frac{\cos(\omega t+\phi)}{\omega(\omega-\omega_b)} \right.$$

$$\left. - \frac{\cos(\omega_b t+\phi)}{\omega_b(\omega-\omega_b)} \right]$$

where $\omega_b = \frac{eB}{m}$ is the cyclotron frequency. Equation 7.2 exhibits a resonance effect at $\omega = \omega_b$ where the electron continuously gains energy from the electric field. A good approximation is given by the equations:

$$(7.4)\quad W = \frac{e^2 E_0}{8m} t^2$$

$$(7.5)\quad \frac{dW}{dt} = \frac{e^2 E_0}{4m} t = \text{power dissipated}$$

We can determine those times t for which x = 0 and $\omega \geq \omega_{MIN}$, where W_{MIN} is the energy for which the secondary emission ratio is unity, by inspection. By requiring that all three numerators on the right side of equation 7.2 be unity, so as to maximize u, we obtain $\phi = -\pi/2, \omega_b t = \pi$ and $\omega = 2n\pi$ where n = 1/2 or an integer. For n = 1/2, which corresponds to cyclotron resonance, we have

$$(7.6)\quad W_{\omega=\omega_b} = \frac{\pi^2}{8} \frac{e^2 E_0^2}{m\omega^2}, \quad \omega t = \pi$$

For n = 1 which corresponds to the experimentally observed glow at $\omega = 2\omega_b$, we have

$$(7.7)\quad W_{\omega=2\omega_b} = \frac{20}{9} \frac{e^2 E_0^2}{m\omega^2}, \quad \omega t = 2\pi$$

The energy given by equation (7.7) is approximately twice that given by equation 7.6. Physically, this arises because the electron has been accelerated twice as long as it was under conditions of equation 7.6. For n = 2, which corresponds to a possible resonance at $\omega = 4\omega_b$, we have

$$(7.8)\quad W_{\omega=4\omega_b} = 0.82 \frac{e^2 E_0^2}{m\omega^2}, \quad \omega t = 4\pi$$

which is somewhat lower than the energy at cyclotron resonance. For n = 3 or more, the energies are smaller still.

For purposes of prediction, we can summarize the results for this case as follows:

1. The excitation frequency must be equal to $2n\omega_b$ where n = 1/2 or an integer and $\omega_b = \frac{eB}{m}$.
2. The energy as given by equation 7.4 for the acceleration time determined by equation 7.3 must be high enough to yield a secondary electron emission ratio greater than one.

The initial velocity of the emitted electrons was set at zero in the preceding analysis to simplify the mathematics. The effect of including initial velocity is to raise the energy given by equation 7.4 by $\frac{k^2}{k^2 - 1}$ (which = 1.125 for k = 3).

Single surface multipacting with parallel electric and magnetic fields was first observed by Priest and Talcott[45] in the heating of output windows in klystrons, and the analysis presented here is due to them. Figure 15 shows the typical electron motions that arise in this case. For an electron emitted from the surface shown in Figure 16, where

U_o is the initial velocity of the electron

E_{RF} is an alternating electric field parallel to the surface

H is a static magnetic field parallel to the surface,

the equations of motion are

$$(7.9)\quad \frac{d^2x}{dt^2} = \frac{e}{m} E_{RF} \sin\omega t$$

$$(7.10)\quad \frac{d^2y}{dt^2} = -\frac{e}{m} H \frac{dz}{dt}$$

$$(7.11)\quad \frac{d^2z}{dt^2} = \frac{e}{m} H \frac{dy}{dt}$$

Solving, subject to the boundary conditions

$$(7.12)\quad \left.\begin{aligned} x = y = z &= 0 \\ \dot{x} = \dot{z} &= 0 \\ \dot{y} &= u_o \end{aligned}\right\} \text{at } t = t_o,$$

Priest found that multipacting was possible when:

(1) The excitation frequency $w = \frac{eH}{m}$ = cyclotron frequency

(2) The arrival energy $W = 2\left(\frac{e}{m}\right)\left(\frac{E_{RF}}{w}\right)^2 + W_o$ (where W_o is the initial energy) is high enough to yield x a secondary emission ratio greater than one, i.e., $W \geq W_{min}$.

For prediction purposes, the second of these conditions can be approximated as:

$$2\left(\frac{e}{m}\right)\left(\frac{E_{RF}}{\omega}\right)^2\left(\frac{k^2}{k^2-1}\right) \geq W_{MIN}$$

where $k = \frac{u}{u_o} \cong 3$ (Gill and von Engel's assumption).

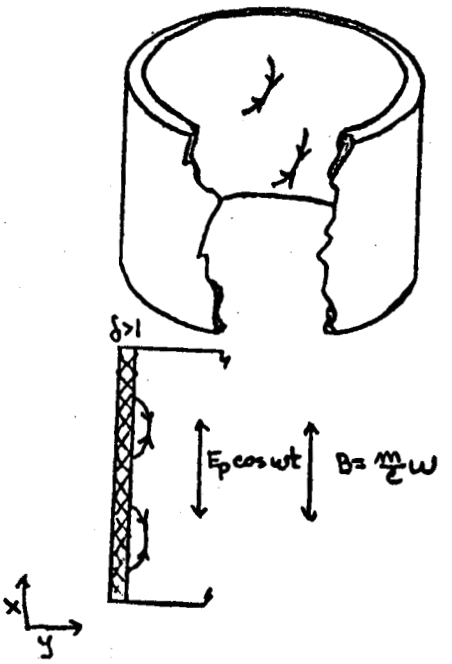

Figure 15. Typical Electron Motions With Axial Magnetic Field Having the Cyclotron Resonance Value, after Priest

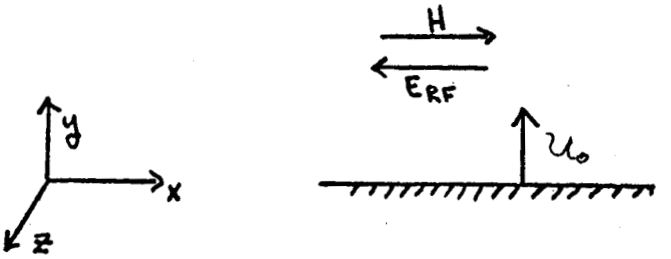

Figure 16. Field and Velocity Relationships in Single Surface Multipacting with Parallel Electric and Magnetic Fields, after Priest.

LOADING DUE TO MULTIPACTING

The energy electrons lose in striking the surfaces must be known in order to calculate how much energy the field must supply and the loading introduced by the multipacting. For the plane parallel plate geometry with $k = u/u_o$ = constant, we have for the energy lost per transit by one electron:

$$(8.1)\quad W = \tfrac{1}{2} m u^2 - \tfrac{1}{2} m u_o^2 = \tfrac{1}{2} m u^2 \left[1 - \frac{1}{k^2}\right]$$

Then, from equation (1.7), we obtain

$$(8.2)\quad W = \tfrac{1}{2} m \left[\left(\frac{k}{k-1}\right)\left(\frac{2eV}{mwL}\cos\phi\right)\right]^2 \left(\frac{k^2-1}{k^2}\right)$$

which reduces to

$$(8.3)\quad W = \tfrac{1}{2} m \left(\frac{k+1}{k-1}\right)\left(\frac{2eV}{mwL}\right)^2 \cos^2\phi$$

Assuming that there are N electrons in each bunch and that a bunch starts from one surface or the other during half each cycle (even in the higher modes, where this would mean that several bunches were in existence at the same time), the power absorbed per second is

$$(8.4)\quad P = 2Nf\,W = \frac{4N(eV)^2 f}{mw^2L^2}\left(\frac{k+1}{k-1}\right)\cos^2\phi$$

This corresponds to an equivalent peak in-phase component of current

$$(8.5)\quad I = \frac{2P}{V} = \frac{8Ne^2Vf}{mw^2L^2}\left(\frac{k+1}{k-1}\right)\cos^2\phi$$

flowing through a resistance

$$(8.6)\quad R = \frac{V^2}{2P} = \frac{\pi m f L^2}{4e^2 N\cos^2\phi}\left(\frac{k-1}{k+1}\right) = \frac{\pi m f L^2}{4e^2 N\cos^2\phi}\left(\frac{k-1}{k+1}\right)$$

This resistance is a convenient way to express the loading effect of multipacting, since it can be compared directly to the shunt resistance of the gap. There is also an equivalent reactance due to the phase of the oscillating electron bunches, but this has been neglected in this report.

To get an idea of the order of magnitude of the loading, consider the case:

$\phi = 18^{\circ}$ $\qquad$ $N = 10^{6}$

$k = 3$ $\qquad$ $d = 0.5$ cm.

$f = 4 \times 10^{8}$ cps.

These are typical values of a situation in which multipacting has been observed, the value for N being the order of magnitude of gain given by Farnsworth. Putting these values into equation (8.6) gives a resistance of 100 ohms absorbing a power of 15 watts. In the particular experimental case, using these dimensions, the power loss was less than that predicted. This is not unexpected; when an actual system is loaded by the multipacting discharge, the voltage tends to drop until the conditions for multipacting are just met. In this marginal condition, N is reduced until the load on the voltage source is small enough to permit stable operation.

Although this analysis has been specifically for the parallel plate geometry, the energy supplied by the r-f field to a multipacting electron in the geometries and electrical conditions discussed thus far is given approximately by

$$W = (k^2-1)E_o = \left(\frac{k^2-1}{k^2}\right)E_{impact} \tag{8.7}$$

where E_o, the average emission energy, and E_{impact}, the impact energy, are functions of the particular multipacting conditions. The power absorbed per second is then

$$P = 2NfW = 2\left(\frac{k^2-1}{k^2}\right)N f E_{impact} \tag{8.8}$$

flowing through a resistance

$$R = \frac{k^2 V_{RF}^2}{2(k^2-1)Nf E_{impact}} \tag{8.9}$$

SECONDARY EMISSION

Multipacting discharge depends critically on the nature of the surface involved because of the requirement that the secondary emission ratio, δ, be greater than one. A simple phenomenological approach is sufficient for our purposes, but more detailed treatments are available. The main feature of interest is the relationship between the secondary emission ratio and the incident electron energy as shown in Figure 17 for a typical material.

The shape of this curve is much the same for all materials with the main differences being in the values of W_f, δ_{max} and W_{max}. Data has been compiled for many common materials and is presented in Table 1. However, for purposes of calculating δ for use in prediction of multipacting, several other factors must be taken into account as follows:

1. The secondary emission ratio is higher for glancing incidence as shown in Figure 18. This means that cases where a stream of electrons is glancing the surface (as in "single-surface multipacting with perpendicular electric fields) will yield a higher δ than given in the table and that a change in geometry to avoid normal incidence will not necessarily eliminate multipacting.
2. The secondary electrons have an energy distribution of the form shown in Figure 19. The effect this has on predictions of multipacting and the final composition of the discharge is discussed at length in the section entitled "Effects of Variations in Electron Velocities."

3. Metallic oxides tend to have a higher δ_{max} and lower W_f than the pure metal, e.g., note comparative values of aluminum oxide vs. aluminum in the table on Page 35. This means that any oxidation of a surface will tend to make multipacting more likely an important consideration in practical devices that may be exposed to oxygen before use in a vacuum. Also, metallic oxides may act as rectifiers (e.g., copper-cuprous oxide) so that a surface charge may form on the oxide surface during multipacting and produce effects much like that of a d-c bias.
4. Organic deposits such as oil on a surface tend to reduce the minimum threshold sharply. For instance, recent data indicates that the W_f for a gold surface may be reduced from 180 volts to approximately 23 volts when an oil film is on the surface. This lowering of W_f by contamination is an important factor in fabrication of r-f components and in vacuum test set-ups (where it is difficult to keep vacuum pump oil from being deposited on the tested equipment).
5. Rough, irregular surfaces tend to reduce the effective δ by making it more difficult for an electron to escape as shown in Figure 20. For this reason, layers of black substances such as soot or black nickel tend to have a lower δ_{max} than the same element in a smooth form as shown in Figure 21. Also, a rough surface has a secondary yield that is nearly independant of the angle of incidence. Unfortunately, these rough surfaces may have undesirable electric characteristics such as a high surface resistance, that would preclude their use.

Table 1

Secondary Emission Characteristics of Common Materials

Material	δ Max.	W, $\delta = \delta_{Max.}$	W_f
Ag	1.5	800	
Al	1.0	300	
Au	1.0	800	125
C	1.0	300	120
Cu	1.3	600	75-175
Fe	1.3	350	125
Ni	1.3	550	125
Co	1.1	500	300
Pb	1.1	450	250
Rb	0.8	400	--
Sn	1.3	500	160
Ag_2O	1.1		
Al_2O_3	2.5	350	20
Cu_2O	1.2		
MgO	2.4	1500	
SnO_2	1.1		
RbO_2	5.8		
NaC_1	6.8	600	15
$SbCs_3$	5-8.3	375	10
Quartz	2.1	400	30
Soda Glass	2.1	300	
Mica	2.4	380	30

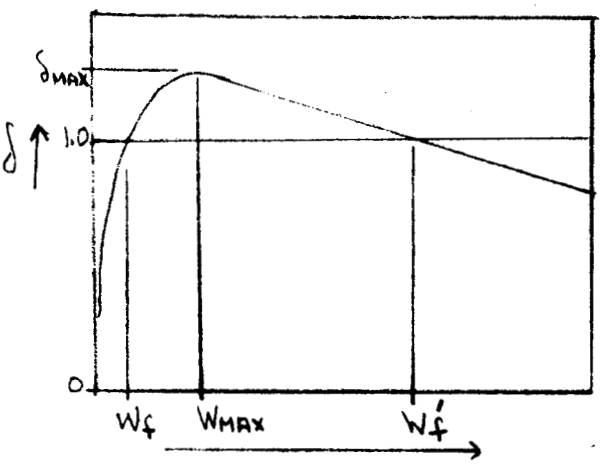

V_p = Incident Electron Energy

Figure 17. Secondary Electron Emission Yield As A Function of Incident Electron Energy

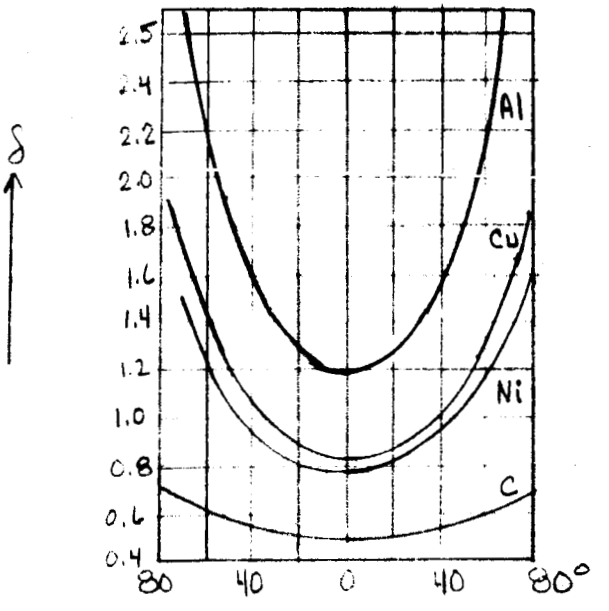

Angle of Incidence O ⟶

Figure 18. Secondary Emission Yield Versus Angle of Incidence of Primary Electrons

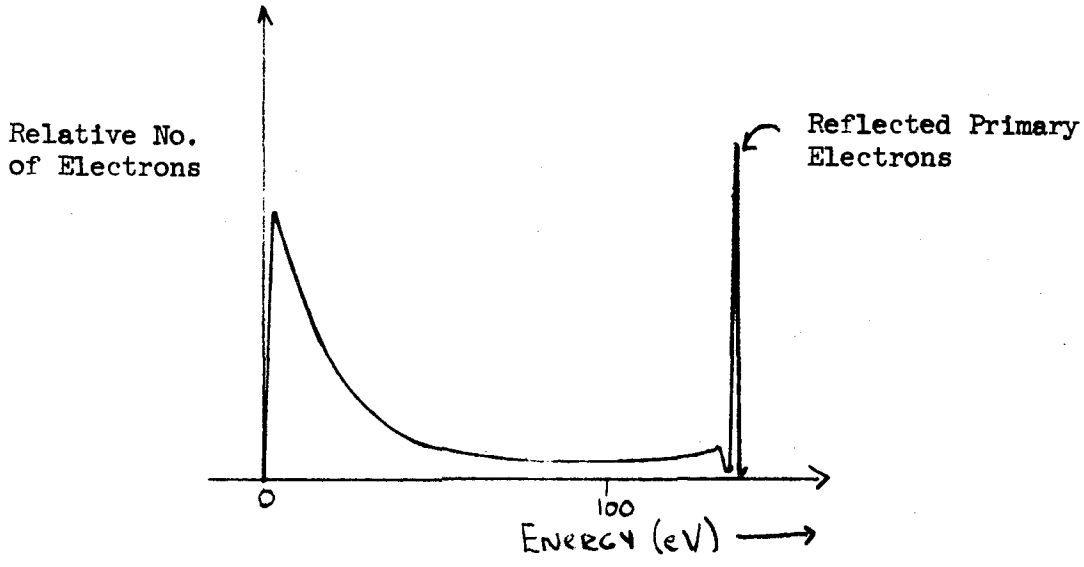

Figure 19. Energy Distribution of Secondary Electrons

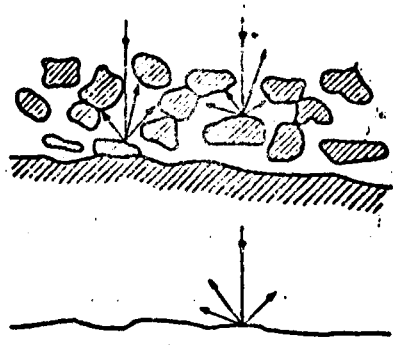

Figure 20. Explanation of the low yield of a "rough" surface; the electron can leave a smooth surface unhindered but with a rough surface it may be intercepted by surrounding walls.

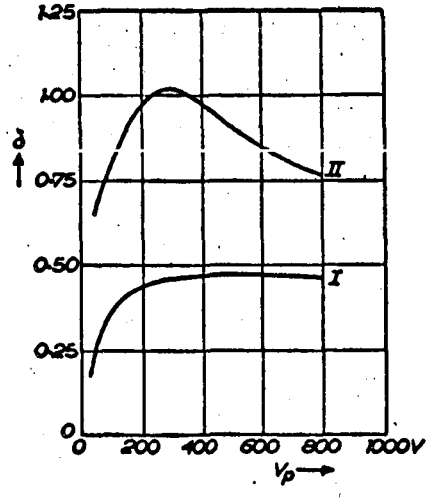

Figure 21. Secondary electron emission yield of soot (I) and of a smooth carbon surface (II); according to Bruining.

EFFECTS CAUSED BY THE VARIATIONS IN INITIAL ENERGIES OF SECONDARY ELECTRONS

Since secondary electrons are emitted with energies that vary considerably (see Figure 19), a variation of transit time will occur. These transit time variations result in a distribution of the secondary electrons over a range of phase angles at the end of a single half period.

In the analysis thus far, it has been assumed that the initial speed u_o of the secondary electrons was different from zero and that the ratio, $u/u_o = k$, was a constant for all the electrons that played a significant role in the discharge. With this assumption, the optimum phase angle for secondary electrons is indeed described by a single value of k; the analysis assigns a single emission phase angle (the optimum one) to the majority of electrons, and since the secondary-electron emission from the electrodes occurs almost instantaneously, it is customary to think of the electrons as crossing the gap in a very thin sheet without phase spreading.

Although the theoretical results obtained using this assumption of constant k have been shown to be in agreement with experiments, it has been pointed out by several observers[12, 18, 41] that the u/u_o ratio could not be a constant for either fixed values of the electrode separation, frequency and peak electric field (Case 1) or along the minimum breakdown potential curve (Case 2). In Case 1, it should be noted that secondary electrons not emitted with the same velocity do not in general reach the opposite electrode with the same u_{impact}/u_o ratios. For Case 2, it is noted that along the minimum breakdown voltage curve, the voltage can be represented by the relation $V \sim f^2 d^2$ where f is the frequency and d is the electrode separation. Since the impact velocity is also proportional to fd, the average value of u in general depends on fd. On the other hand, the average value

of U depends only slightly on U_o. Consequently, the ratio U/U_o is ordinarily different for distinct choices of fd along the minimum breakdown voltage curve. In spite of these objections, the theoretical results obtained using that assumption have been shown to be in good agreement with experiments.

Recent theoretical work[41] has indicated that the interaction of phase angles and emission velocities is such that the assumption of constant k gives essentially correct results even though U/U_o is not constant for all of the secondary electrons. By using a digital computer to perform the calculations, Miller was able to make a detailed study of the motion of a large number of electrons over several successive half cycles in which the spread of phase angles and emission velocities was taken into account.

Investigation of the steady state configuration reached by the electron groups showed the following

1. The assumption U/U_o = constant has a theoretical basis in that the steady state multipacting electron distribution with respect to $k = \bar{U}/\bar{U}_o$ is rather narrow and shows a peak near the semiempirically determined value of k = 3 for the minimum breakdown field strength.
2. The behavior of the most probable phase angle and the overall distribution of phase angles were in excellent agreement with the values predicted on the basis of the simple theory developed earlier in this report.

THE EFFECTS OF GAS ATOMS ON THE MULTIPACTING MECHANISM

For gas pressures of 10^{-3} to 10^{-5} Torr, a considerable amount of ionization occurs within a multipacting discharge chamber in spite of the fact that the electron mean free path* is ten or twenty times greater than the electrode separation. There are two principal reasons for this. In the first place, although the electron currents are in the range of milliamperes, this represents a fairly large number of electrons in comparison with the density of the gas atoms present. Hence, one might expect that a substantial amount of ionization would be observed, and indeed, a faint glow has been observed down to 10^{-6} Torr.

Second, the positive ions formed tend to aid in further ionization. Williams has shown that the large numbers of slow moving electrons near the electrodes create an electric field that directs the positive ions to the center of the discharge region. When trapped in this potential well at the center, the gas atoms can become multiply ionized through further collisions with electrons. Since the multipacting electrons have an appreciable velocity in the center region, recombination is less likely there than at the surfaces of the electrodes where the emitted electrons are moving slowly.

The collisions between the multipacting electrons and the gas atoms tend to retard the buildup of the multipacting current by removing a certain percentage of the electrons from the group, since the colliding electrons are essentially lost to the process. As the electron current builds up, as determined primarily by the yield ratio of the electrode material, more and more ions are created by the collisions between the electrons and

* The electron mean free path in air at $0^{\circ}C$ = 7.13×10^{-4}/cm/pressure in mm. of Hg (from Cobine).

gas mclecules. When the ions collect at the center of the region as outlined above, they can have important effects on the dynamics of the electrons.

The effect of the positive ion cloud is to reduce the electron transit times by providing additional acceleration during the early portion of the electron flight and de-acceleration just before the electron strikes the opposite electrode. In effect, the ion cloud may cause a detuning of the electron phases, a detuning which increases as the density of the ion cloud increases. Recent observations by Miller[41] indicate that this detuning can result in sizable low frequency pulsations in the multipacting current as well as being a significant factor in the very sharp cutoff of multipacting along the upper and lower breakdown curves.

The presence of gas atoms may also lead to the existence of other effects that may be mistaken for multipacting. Principal among these is sparkover and corona. Sparkover[11] occurs in parallel plate cases and in coaxial cylinder configurations where the ratio of outside to inside diameters is less than 2.72. The minimum voltages at which sparkover occurs is given approximately by Paschen's law as summarized in the table below.

	Minimum Voltage	Optimum pd Froduct (Pressure in cm. of Hg x gap spacing in cm.)
Air	341	5.7
Helium	261	27
Nitrogen	251	6.7

The minumum voltage is smallest for the optimum pd product. A further correction must be added for high frequency operation, e.g., reduce voltages 10% at 900 kc.

Corona[11] occurs when the ratio of outside-to-inside diameters in greater than 2.72 with the minimum voltage given approximately by

$$(11.1)\quad V_c = 31 m \delta \left[1 + \frac{.308}{\sqrt{\delta a}}\right] a \ln b/a$$

where

a = inside radius

b = outside radius

δ = relative air density factor = $\frac{3.92}{273 + t}$

m = irregularity factor. Usually 1 for smooth surfaces.

p = barometric pressure in cm of Hg.

t = temperature ^{o}C.

APPENDIX - PART IV

PART IV

BIBLIOGRAPHY

BIBLIOGRAPHY

1. Abraham, W. G., "Interactions of Electrons and Fields in Cavity Reasonators," Ph.D. dissertation, Stanford University, Stanford, Calif.; 1950

2. Agarwal, B. K., "Variation of Secondary Emission with Primary Electron Engergy," Proc. of the Physical Society, vol. 71, pp 851-852; 1958

3. Aitken, D., "Long Transit Time Multipactoring at UHF and the Effects of Surface Emitting Lavers," Proc. of IEE; May 1958

4. Baller, H. H. and Phillips, E. V., "Investigations of Failures of Wideband OAO Transmitter in Vacuum Test," Hughes Aircraft Co., Report No. TM-756; July 1963

5. Bol, Kees, "The Multipactor Effect in Klystrons," 1954, IRE National Convention Record, vol. 2, pt, 3, pp 151-155

6. Bondley, R., "Secondary Emission Suppression in Electron Beam Tubes," U. S. Patent No. 2,955,229; Oct. 4, 1953

7. Brown, S. C., "Basic Data on Plasma Physics," Technology Press, MIT, Cambridge, Mass.; p 214; 1959

8. Bruining, H., "Physics and Applications of Secondary Emission," New York; 1954

9. Clifford, D. S., "Failure of Vacuum Insulation at Low Field Strengths," Nature; vol. 170; p 503; 1952

10. Clothieux, E., "Ion Confinement in a Gas Discharge Controlled by Secondary Electron Resonance," Ph.D. Thesis, New Mexico State University, University Park, New Mexico; January 1963

11. Cobine, J., "Gaseous Conductors," Dover; New York; 1958

12. Fang, F., "Secondary Electron Multiplication in Microwave Field," Univ. of Ill., Urbana, Ill., Scientific Report No., Contract AF 19(604)-2152; May 15, 1959

13. Farnsworth, P. T., "Television by Electron Image Scanning," Journal of the Franklin Institute; Vol. 2; p 411; 1934

14. Forrer, M. P., "Study of Multipactor Discharge Characteristics," Palo Alto, California, General Electric Co. Report No. R59ELM-158, Contract AF 30(602)-1641; June 1959

Bibliography (Continued)

15. Forrer, M. and Milazzo, C., "Duplexing and Switching with Multipactor Discharges," Proc. of the IRE, V. 50; n. 4; pp 442-450; April 1962

16. Francis, G. and van Engel, A., "The Growth of the High Frequency Electrodeless Discharge," Philosophical Transactions of the Royal Society of London; Series A; Vol. 246; pp 143-80; 1953

17. Gill, E. W. B. and Donaldson, R. H., "The Sparking Potentials of Electrodeless Discharges," Philosophical Magazine and Journal of Science; Vol. 12; p 719; 1931

18. Gill, E. W. B. and van Engel, A., "Starting Potentials of Electrodeless Discharges," Proceedings of the Royal Society of London; Vol. 192; p 446-463; 1948

19. Greenblatt, M., "A Microwave Secondary Electron Multiplier," Review Science Instruments; Vol. 20; p 646; 1949

20. Gutton, C., "Electric Discharge at Very High Frequency," Campes Rendus hebdormadaires des seances de l' academie des sciences; Vol. 178; p 467; 1924

21. Gutton, C., and Gutton, H., "Electric Discharge at Very High Frequency," Comptes rendus hebdomadaires des seances de l'academie des sciences, Vol. 186; p 303; 1928

22. Hackenburg and Brauer, "Secondary Electron Emission from Solids," Advances in Electronics and Electron Physics; Vol. 11; New York; 1959

23. Hatch, A. J., "Electron Bunching in the Multipacting Mechanism of High Frequency Discharge," Journal of Applied Physics; Vol. 32, N. 6; pp 1086-1092; 1961

24. Hatch, A. J., "Radio Frequency Fields in rf Plasmas and Plasmoids," Bulletin of the American Physical Society; Vol. 5; p 152; 1959

25. Hatch, A. J., "Multipacting Modes of High Frequency Gaseous Breakdown," The Physical Review; Vol. 112; pp 681-685; 1958

26. Hatch, A. J., "High Frequency Plasmoids," Gaseous Electronics Conf., Argonne National Lab., Lemont, Ill.; 1958

27. Hatch, A. J., "Plasma Studies in a Low Pressure High-Frequency Discharge," Argonne National Lab., Lemont, Ill., Geneva Conference Paper No. 351; 1958

28. Hatch, A. J. and Williams, H. B., "The Secondary Electron Resonance Mechanism of Low Pressure-High Frequency Breakdown," The Journal of Applied Physics; Vol. 25; pp 417-423; 1954

Bibliography (Continued)

15. Forrer, M. and Milazzo, C., "Duplexing and Switching with Multipactor Discharges," Proc. of the IRE, V. 50; n. 4; pp 442-450; April 1962

16. Francis, G. and van Engel, A., "The Growth of the High Frequency Electrodeless Discharge," Philosophical Transactions of the Royal Society of London; Series A; Vol. 246; pp 143-80; 1953

17. Gill, E. W. B. and Donaldson, R. H., "The Sparking Potentials of Electrodeless Discharges," Philosophical Magazine and Journal of Science; Vol. 12; p 719; 1931

18. Gill, E. W. B. and van Engel, A., "Starting Potentials of Electrodeless Discharges," Proceedings of the Royal Society of London; Vol. 192; p 446-463; 1948

19. Greenblatt, M., "A Microwave Secondary Electron Multiplier," Review Science Instruments; Vol. 20; p 646; 1949

20. Gutton, C., "Electric Discharge at Very High Frequency," Campes Rendus hebdormadaires des seances de l' acadamie des sciences; Vol. 178; p 467; 1924

21. Gutton, C., and Gutton, H., "Electric Discharge at Very High Frequency," Comptes rendus hebdomadaires des seances de l'acadamie des sciences, Vol. 186; p 303; 1928

22. Hackenburg and Brauer, "Secondary Electron Emission from Solids," Advances in Electronics and Electron Physics; Vol. 11; New York; 1959

23. Hatch, A. J., "Electron Bunching in the Multipacting Mechanism of High Frequency Discharge," Journal of Applied Physics; Vol. 32, N. 6; pp 1086-1092; 1961

24. Hatch, A. J., "Radio Frequency Fields in rf Plasmas and Plasmoids," Bulletin of the American Physical Society; Vol. 5; p 152; 1959

25. Hatch, A. J., "Multipacting Modes of High Frequency Gaseous Breakdown," The Physical Review; Vol. 112; pp 681-685; 1958

26. Hatch, A. J., "High Frequency Plasmoids," Gaseous Electronics Conf., Argonne National Lab., Lemont, Ill.; 1958

27. Hatch, A. J., "Plasma Studies in a Low Pressure High-Frequency Discharge," Argonne National Lab., Lemont, Ill., Geneva Conference Paper No. 351; 1958

28. Hatch, A. J. and Williams, H. B., "The Secondary Electron Resonance Mechanism of Low Pressure-High Frequency Breakdown," The Journal of Applied Physics; Vol. 25; pp 417-423; 1954

Bibliography (Continued)

29. Hoover, V. and Smither, R., "Secondary Electron Resonance Discharge Mechanism," Physical Review; Vol. 98; p 1149; 1955

30. Jenny, D. A., "Secondary Electron Emission at High-Current Densities," Ph.D. dissertation, Swiss Federal Institute of Technology, Zurich, Switzerland; 1951

31. Jet Propulsion Labratories, "The Lunar Program," Space Programs Summary No. 37-21; May 1963

32. Kanichcua, I., and Burtsev, V., "Electron Penetration with Energies from 0.5 to 16 kev thru Collodium and Goldfilms," Soviet Physics - Solid State; Vol. 1; pp 1146-1152; 1959

33. Krebs, K., "Frequenzvervielfachung im Zentimeterwellengebiet durch Sekundarelektronen," Z. Physik; Vol. 154; pp 19-26; January 1959

34. Krebs, K., "Pendalvervielfachung von Sekundar Elektronen in Hochfrequenzfeldern," Z. Angew Phys.; Vol. 2; pp 400-411; October 1950

35. Krebs, K. and Meerbach, M., "Die Pendelvervielfachung von Sekundarelektronen," Ann. Physik; Vol. 15; No. 3-4; pp 189-206; 1955

36. Krebs, K. and Meerbach, M., "Die Elektronendichte und Geschwindigkeitsverteilung bei der Pendelvervielfachung von Sekundarelectronen," Ann. Physik, Vol. 18; pp 146-162; August 1956

37. Krebs, K. and Villiz, H., "Die Auregung von Hohlraumresonatoren durch Pendelvervielfachung von Sekundarelectronen," Z. Physik; Vol. 154; pp 27-33; January 1959

38. McKay, K. G., "Secondary Electron Emission," Advances in Electronics; Vol. 1; Academic Press, N. Y.; pp 65-132; 1948

39. Mevers, L. M., "Electron Optics, Theoretical and Practical," Van Nostrand; pp 306-325; 1939

40. Milazzo, C., "Study of Multipactor Discharge in the Presence of a D-C Bias," Palo Alto, California, General Electric Co. Tech. Memo TM-61-15; March 1961

41. Miller, A., "Experimental and Theoretical Investigations of the Secondary Electron Emission Phase Distributions in a Low Pressure Multipacting Discharge," Ph.D. Thesis, New Mexico State University, University Park, New Mexico; June 1961

42. Mullett, L. M., Clay, R., and Hadden, R., "Multipactor Effect in Linear Accelerators and Other Evacuated R-F Systems and a New Cold Cathode Valve," Atomic Energy Research Establishment Harwell, Berkshire, Report No. GP/R 1076; September 1953

Bibliography (Continued)

43. Murdock, C., Priest, D. and Woeren, J., "High Power Klystrons at U.H.F.," Proceedings of IRE, No. 41, pp 20-35, Jan. 1953

44. Nanevicz, J., "Study of Radiation and Reception of Electromagnetic Energy from Aircraft and Guided Missiles," Monthly Progress Letters 8-10; Contract AF 19(628)-325; Stanford Research Institute

45. Preist, D. and Talcott, R., "On Heating of Output Windows of Microwave Tubes by Electron Bombardmentm"; IRE Trans. on Electron Devices; Vol. ED-9; pp 405-410; September 1962

46. Shul'man, A. R., Zakiyova, I. R., Morozov, Yu. A., and Fridrikhov, S. A., "The Secondary Electron Emission of Nickel," Zhurnal Tekhnicheskoi Fiziki, Vol. 28, p 87; 1958

47. Skobel, F., Report Number 5221-1122; Sperry Gyroscope Company, Great Neck, N. Y.; October 1948

48. Sperry Gyroscope Co., "Final Report on the Multipactor Study Program"; Great Neck, N. Y.; Contract No. nr-217(01); Report No. 5270-6144; October 1953

49. Talcott, Ruth, "The Effects of Titanium Films on Secondary Electron Emission Phenomena in Resonant Cavities and at Dielectric Surfaces," IRE Trans. on Electron Devices; Vol. ED-8; pp 243-251; July 1961

50. Tamagawa, H., Electro-Technic Journal of Japan; Vol. 3 n. 2; pp 42-46; June 1957

51. Tamagawa, H., "A Theory of High-frequency Discharge in High Vacuum," Electrotechnical Journal of Japan; Vol. 3, No. 3; pp 93-97; September 1957

52. Vance, E. F. and Nanevicz, J. E., "One Sided Multipactor Discharge Modes," SRI Report No. 75; Contract AF 19(628)-325; April 1963

53. Williams, H. B., "Three-Dimensional Potential Well," The Physical Review; Vol. 107; p 1451; 1957

54. Wood, R. W., "Plasmoidal H. F. Oscillatory Discharges in Non-Conducting Vacua," The Physical Review; Vol. 35; p 673; 1930

55. Zworykin, V., Reudy, J. and Pike, E., "Silver magnesium alloy as a secondary emitting material," Journal of Applied Physics; Vol. 12; pp 696-698; September 1941

56. "Multipactor Breakdown in Space Electronic Systems", Hughes Aircraft Company, Report TP-412, November 1963. Technical Proposal.

57. F. Fossel and K. Krebs, "Die Pendelvervielfachung von Sekunparelektronen Als Zundbedingung von Hochfrequenzladung", Aeitschrift Fur Physik, V.175 p382-390, 1963.

58. Vance, E. F., Journal of Applied Physics, V.34, 11 November 1963.

59. Hayes, R., Ertel MacCulough Co., Report on Project Defender, Cont. DA36(039)SC90818, July 1962-June 1964, "Research on Microwave Window Multipactor and its Inhibition."